A Multi-objective Optimization Method for Industrial Park Layout Design – the Trade-off between Economy and Safety

Ruiqi Wang[a,b], Yufei Wang[a], Truls Gundersen[b], Yan Wu[c], Xiao Feng[c], Mengxi Liu[a]

a State Key Laboratory of Heavy Oil Processing, China University of Petroleum, Beijing, 102249, China

b Department of Energy and Process Engineering, Norwegian University of Science and Technology (NTNU), Trondheim, NO-7491, Norway

c School of Chemical Engineering and Technology, Xi'an Jiaotong University, Xi'an, Shaanxi, 710049, China

Abstract

The general layout design significantly impacts the economy and safety performance of an industrial park. In most of the previous works about the industrial facility layout problem (FLP), safety issues are converted to economic numbers in objective functions. However, this conversion is not appropriate, and the results cannot guide the trade-off between economy and safety. In this work, a multi-objective optimization method for industrial park layout is proposed to obtain a set of solutions (Pareto curve) that achieves different trade-offs between economy and safety. Total capital cost and expected fatalities are selected as the two objectives. An improved FLUTE algorithm is employed to obtain the most economical pipe networks. In terms of safety, an extended risk map method is proposed to describe the distribution of risk considering the uncertainty of weather conditions. The proposed model is compared with a single-objective method in one case study to show the superiority of the proposed method. In addition, three different evolutionary algorithms are employed to solve a second case for comparison. The results show that the non-dominated sorting genetic algorithm – II (NSGA-II) is more effective for industrial FLPs with multi-objective.

Key words: Industrial park; Layout; Multi-objective optimization; Safety evaluation; Pareto curve

1 Introduction

The facility layout problem (FLP) is to determine the physical organization of a production system[1]. For process industries, it means to determine the locations of plants in an industrial park or the locations of facilities in a plant. A proper arrangement of plants and facilities contributes to land saving, pipe material saving, and risk reduction. Therefore, layout optimization can significantly improve the performance of both economy and safety of the enterprise[2], and this is also the reason why the FLP has attracted extensive attention from researchers during recent decades[3]. According to statistics[4], material handling contributes about 20%-50% of the operating cost in manufacturing, and 10-30% of such costs can be saved by implementing an efficient layout.

FLPs can be classified into two categories: grid-based model and continuous model; sometimes they are called equal area facility layout problem (EA-FLP) and unequal area facility layout problem (UA-FLP)[5]. In grid-

based models, the free space is divided into several grids with same sizes, and each facility can occupy one or more grids. If occupying one grid, such a problem can be considered as an assignment problem to distribute facilities to several pre-defined locations without the consideration of shape and dimension of facilities, while occupying more grids usually leads to a more complex formulation[6]. Martinez-Gomez et al.[7] proposed a method to optimize the layout of a plant based on the grid model, in which a facility can occupy several grids. A risk map is also used in their work to describe the risk in every grid. However, in most applications and practice, basing the layout on grids is a very poor assumption[8]. In continuous models, the coordinates of the facilities can vary continuously, and the shapes and dimensions of the facilities are also considered. Therefore, non-overlapping constraints should be included in such kind of models. However, non-overlapping constraints are usually difficult to deal with. Penteado and Ciric[9] proposed a model to optimize the layout of a plant. Their work is relatively comprehensive and early for industrial facility layout. The objective function consists of pipe cost, land cost, protection device cost, and financial risk. A pre-defined minimum distance between every two facilities is used to handle the non-overlapping constraints. Our method uses a continuous model to make it more practical.

Pipe network is an important factor to consider for industrial parks. Most research on the industrial facility layout problem has considered land cost, pipe cost (simple pipe) and risk cost, while the cost of pipe networks is neglected. A simple pipe refers to a pipe only connecting two plants to transport materials. In contrast, a pipe network has several branches connecting several plants, for example steam pipe networks and hydrogen pipe networks. Pipe networks exist widely in industrial parks. Alnouri et al.[10] proposed a method to merge common pipe segments in water reuse networks to reduce capital cost. Wu and Wang[11] first defined the problem of pipe network arrangement and then proposed a systematic method based on the Kruskal algorithm[12] to solve it. Their approach can find the shortest arrangement for a pipe network to connect several plants. However, the method is extremely expensive in calculation time. Later, Wang et al.[13] and Wu et al.[14] accelerate the solution process significantly by implementing the FLUTE algorithm[15] and the GeoSteiner algorithm[16], respectively. However, the methods mentioned above can only find the shortest routing for a pipe network, rather than the most economical routing. Wang et al.[17] improved the FLUTE algorithm to find the most economical routing. They found that in approximately two-thirds of the situations, the shortest routing is not the most economical routing, and the pipe network cost can be reduced by up to 38%. The improved FLUTE algorithm is implemented in this work to obtain the pipe network cost.

Countless accidents have proved the critical role of safety in industrial processes, and this is the point that distinguishes industrial FLPs from other FLPs. The Center for Chemical Process Safety (CCPS) of the American Institute of Chemical Engineers (AIChE) has many publications to guide the layout design for industrial processes considering safety[18]. However, these guides are heuristic and cannot be used to determine a specific layout scheme. The method of quantitative risk analysis (QRA) is widely employed in academic research to measure risk. Therefore, many safety evaluation methods are introduced in the studies of industrial FLPs. Latifi et al.[19] applied the Pasquill-Gifford model to calculate the concentration of toxic gas in a plant area and determine the layout. The Dow Fire and Explosion Index[20] (Dow F&EI) system is a useful tool to identify hazardous equipment. Patsiatzis et al.[21] proposed a method to design the layout for a plant based on the Dow F&EI. The model provided the possibility to choose different protection devices, which will lead to a different protection device cost and hazard defending effect. The Domino hazard index[22] (DHI) is used to evaluate the hazard related to potential domino effects. Lira-Flores et al.[23] proposed a model based on the DHI to optimize the layout of a plant. The objective function is composed of the capital cost related to layout and the domino escalation cost obtained from the DHI. The consideration of domino effects in industrial facility layout problems is also a kind of implementation of inherent safety. Besides, some

commercial safety evaluation software tools were also employed. Jung et al.[24] optimized the layout of a plant based on the safety evaluation results from the TNT (trinitrotoluene) equivalent model. The flame acceleration simulator (FLACS) was used to study the explosion scenario in 3-dimension for the optimized layout. The FLACS can calculate the overpressure in any location of the plant considering the congestion and confinement effects so that more comprehensive risk information can be provided. The meteorological condition determines the distribution of toxic gas in an industrial area when a toxic release occurs. Most research only consider the wind speed and direction of maximum annual frequency. However, the probability of other meteorological conditions should also be considered. Vázquez-Román et al.[25] proposed a method to process meteorological data to consider the uncertainty of weather for industrial FLPs. However, their approach may generate invalid meteorological parameters that cannot exist in practice. In this work, the method proposed by Vázquez-Román et al. is improved and extended to generate a composite risk map considering the uncertainty of meteorology and various potential accidents.

In the aspect of solution method, both mathematical programming methods and meta-heuristic algorithms are applied. Mathematical programming methods, which are usually based on General Algebraic Modeling System (GAMS), are fast to solve, but the user will suffer from a difficult problem and constraint formulation. Meta-heuristic algorithms are easy and flexible in model construction, but they are time consuming. Guirardello and Swaney[2] proposed a mixed integer linear programming (MILP) model. The model integrated a piping layout superstructure, in which the routing of pipes in 3-dimension can be determined. Caputo et al.[26] applied a genetic algorithm (GA) to optimize the layout of a process plant considering potential explosions. Their work demonstrated the step by step process of GA to find the optimal solution. Alves et al.[27] used a Simulated Annealing (SA) algorithm to optimize the layout of several facilities in a plant to minimize the impact on the nearby residential area.

Single-objective optimization was applied in most of the previous works about industrial FLPs. Safety issues were converted to economic numbers and integrated into the objective function. The conversion is implemented by counting compensation for dead or injured workers in the objective function or considering property loss only and neglect casualties of people. However, this will lead to three severe problems: (1) it is unethical to measure human life with money; (2) it is hard to measure the environmental and social impact of accidents by economic factors; (3) only a specific layout can be obtained from the previous methods based on single-objective optimization, rather than a series of solutions with different economy and safety levels, from which the preferred solution can be selected. Some scholars think safety should be considered as constraints and design the layout on the premise of safety. However, the problem is how to define “safety”. There is no absolute safety, instead, “safety” could be understood as acceptable risk. It should be the designer who determines what an “acceptable risk” is. Therefore, safety should be treated as an independent objective, as important as the economy, and an excellent layout design method should provide the designer with a set of solutions and the flexibility to achieve different trade-offs between economy and safety. Multi-objective optimization seems to be the only way for such kind of dilemmatic problems. However, very few works about industrial FLPs have applied multi-objective optimization. As far as we know, only Martinez-Gomez et al.[7, 28] proposed a multi-objective mixed integer linear programming (MO-MILP) model for industrial FLPs. The total annualized cost and the number of expected fatalities were chosen to be the two objectives. However, since the method was based on an MO-MILP model, the Pareto curves obtained were composed of only a few points and cannot represent the true Pareto front. In our work, a meta-heuristic multi-objective optimization algorithm is used, by which a large number of solutions can be generated to try to approach the true Pareto front. Additionally, the safety evaluation method in our work is improved.

For multi-objective optimization (MOO) problems, evolutionary multi-objective optimization (EMO) algorithms have been significantly developed in recent years. Non-dominated sorting genetic algorithm II (NSGA-II)[29] and multi-objective particle swarm optimization (MOPSO)[30] are two common algorithms based on the classical GA[31] and the particle swarm optimization (PSO)[32] with single-objective. Direct multi-search (DMS)[33] is an improvement of the direct search algorithm specifically for multi-objective optimization. It uses the concept of Pareto dominance to maintain a list of non-dominated points. Besides, the Pareto envelope based selection algorithm II (PESA-II)[34] and the strength Pareto evolutionary algorithm II (SPEA-II)[35] are also two types of EMO algorithms. Additionally, mathematical programming methods based on GAMS can also be implemented in MOO problems with the help of the constraint method. The constraint method means to convert the multi-objective problem to a series of single-objective problems. One of the objectives is selected to be minimized, while the others are treated as constraints. The Pareto front can be obtained by iteratively varying the constraint values of the bound of the other objectives. However, this method cannot deal with complex problems, and the Pareto curve obtained is less likely to be the true Pareto front, similar to the case with Martinez-Gomez et al[28] mentioned above. Some algorithm comparisons were also conducted in the literature mentioned above. However, these comparisons were based on universal mathematical models rather than industrial FLPs specifically. In this work, NSGA-II, MOPSO, and DMS are employed to solve the proposed model for comparison. In Section 6, the reason why NSGA-II is better than MOPSO and DMS for industrial FLPs is also explored.

In this work, multi-objective optimization is implemented to solve industrial FLPs. The total capital cost and the annual number of expected fatalities are the two objectives. Accidents of explosion and toxic release are considered in an extended risk map method. A meteorological data processing method[25] is improved and implemented to consider the uncertainty of meteorological conditions. Finally, the proposed method can provide the designer with a set of solutions and thereby the trade-off between economy and safety can be studied. In the first case, the proposed method is compared with a method from literature[25] by solving the same example , which illustrates the advantage of the proposed model compared with classical models with single-objectives. The second case is a comprehensive case to show all the functions of the proposed method. In addition, in Section 6, different EMO algorithms are implemented for comparison to find the most effective algorithm for multi-objective industrial FLPs. Two other cases are used to illustrate the reason why NSGA-II is more appropriate.

2 Problem statement

This work aims to provide designers with a set of solutions for layout that achieve different trade-offs between economy and safety. A multi-objective optimization model minimizing total capital cost and expected annual fatalities is implemented. A decision maker can determine which layout should be implemented by balancing economy and risk based on the obtained Pareto curve.

The plants are treated as rectangles with different dimensions. Plants can be placed anywhere within the free space, and the boundaries of the industrial park will be determined based on the most distant plants. The situation when the locations of some plants have been determined in advance and cannot be moved is allowed. Plants cannot overlay each other. Therefore, non-overlapping constraints are involved. Both simple pipes connecting only two plants and pipe networks connecting several plants are considered. All pipes should be arranged rectilinearly, i.e., pipes can only go horizontally or vertically.

In the aspect of safety, two kinds of frequent accidents, explosion and toxic release, are considered in the

proposed extended risk map method. The TNT equivalent model and the Pasquill-Gifford model are employed to evaluate the probabilities of death for workers and structural damage for buildings, based on which the composite risk map is generated. The local meteorological data from several years are used in this generation process.

One of the two objective functions is the total capital cost relative to layout, which is composed of land cost, pipe network cost, simple pipe cost, and expected property loss from explosion accidents. The other objective function is the expected annual fatalities.

Therefore, the problem is defined as follows:

Given:

- Coordinates of fixed plants (if existing) (x_1, x_2 ……x_f, y_1, y_2 …… y_f);
- Dimensions of every plant ($L_{l,i}$, $L_{s,i}$);
- Number of workers in every plant ($N_{person,i}$);
- Capital cost of every plant ($U_{plant,i}$);
- Mass and heat of explosive material in every explosive plant (M, ΔH_c);
- Leakage rate of toxic gas in every toxic plant (Q);
- Simple connections between plants;
- Plants that should be connected by pipe networks;
- Unit price for all pipe types with different diameter (U_{simple}, $U_{network}$);
- Meteorological data from several years for the place where the industrial park is located;
- Minimum distance between plants for necessary greenbelt and road (d);
- Available space to accommodate the industrial park ($x_{upper,bound}$, $x_{lower,bound}$, $y_{upper,bound}$, $y_{lower,bound}$);

Determine:

- A set of solutions for layout which achieves different trade-offs between economy and risk.

For each solution, the following variables should be determined:

- Coordinates of every movable plant (x_i, y_i);
- Orientation of every movable plant (z_i);
- Arrangement of every pipe network and the diameters of pipe segments in the pipe network.

Objectives:

- Minimize the total capital cost related to layout (C_{total});
- Minimize the expected annual fatalities (F_{total}).

3 Methodology

3.1 Objective function

Multi-objective optimization is implemented in this work. Therefore, there are two objective functions. One refers to the economy and is composed of land cost, pipe network cost, simple pipe cost, and expected property loss, while the other relates to risk and is the expected annual fatalities from explosion and toxic release accidents. The two objective functions are expressed by Eqs. (1) and (2).

Objective function 1:

$$\text{Min } C_{total} = C_{land} + C_{network} + C_{simple} + C_{property} \tag{1}$$

Objective function 2:

$$\text{Min } F_{total} = \sum_{i=1}^{n_{plant}} P_{death,i} N_i \tag{2}$$

Here, C_{total} is the total capital cost related to layout ($), C_{land} is the land cost ($), $C_{network}$ is the pipe network cost ($), C_{simple} is the simple pipe cost ($), $C_{property}$ is the expected property loss ($), F_{total} is the expected annual fatalities (person/yr), $P_{death,i}$ is the annual probability of death in plant i (/yr), N_i is the number of workers in plant i, and n_{plant} is the number of plants.

3.2 Orientation

Plants should be allowed to rotate to achieve the optimal solution. A binary variable is used to indicate the orientation of a plant, as is expressed by Eqs. (3) and (4).

$$L_{x,i} = z_i L_{l,i} + (1 - z_i) L_{s,i} \tag{3}$$

$$L_{y,i} = (1 - z_i) L_{l,i} + z_i L_{s,i} \tag{4}$$

Here, z_i is a binary variable that indicates the orientation of plant i, $L_{l,i}$ and $L_{s,i}$ are the lengths of the long and short edge of plant i respectively, and $L_{x,i}$ and $L_{y,i}$ are the edge lengths of plant i parallel to the x-axis and y-axis respectively (m).

When $z_i = 1$, the long edge of plant i is parallel to x-axis; when $z_i = 0$, the long edge of plant i is parallel to y-axis.

3.3 Non-overlapping constraints

Two plants cannot occupy the same piece of land. Therefore, non-overlapping constraints are involved. A new non-overlapping constraint is applied in this work, which measures the violation by the coordinates of plants directly. A positive value for at least one value of the distances ($D_{x,i,i'}$ and $D_{y,i,i'}$) means the two plants do not overlap. The formulations are shown in Eqs. (5) - (7).

$$D_{x,i,i'} = \left| x_i - x_{i'} \right| - \frac{(L_{x,i} + L_{x,i'})}{2} \tag{5}$$

$$D_{y,i,i'} = \left| y_i - y_{i'} \right| - \frac{(L_{y,i} + L_{y,i'})}{2} \tag{6}$$

$$\max(D_{x,i,i'}, D_{y,i,i'}) \geq d \tag{7}$$

Here, x_i, y_i, $x_{i'}$, and $y_{i'}$ are the coordinates of the central point of plant i and i', d is the minimum distance between the two plants for necessary road and green belt (m), $D_{x,i,i'}$ is the horizontal distance between the boundaries of the two plants(m), and $D_{y,i,i'}$ is the vertical distance (m).

3.4 Land cost

The land cost is related to the park area, which is expressed by Eq. (8). The park is assumed to be a rectangle. The four boundaries of the park are determined by the most distant plants, as is shown by Eqs. (9) - (13).

$$C_{land} = A_{park} \times U_{land} \tag{8}$$

$$A_{park} = (x_{upper} - x_{lower}) \times (y_{upper} - y_{lower}) \tag{9}$$

$$x_{upper} = \max(x_i + \frac{L_{x,i}}{2}) + \frac{d}{2} \quad i = 1,2,3.....n_{plant} \tag{10}$$

$$x_{lower} = \min(x_i - \frac{L_{x,i}}{2}) - \frac{d}{2} \quad i = 1,2,3.....n_{plant} \tag{11}$$

$$y_{upper} = \max(y_i + \frac{L_{y,i}}{2}) + \frac{d}{2} \quad i = 1,2,3.....n_{plant} \tag{12}$$

$$y_{lower} = \min(y_i - \frac{L_{y,i}}{2}) - \frac{d}{2} \quad i = 1,2,3.....n_{plant} \tag{13}$$

Here, A_{park} is the area of the industrial park (m^2), U_{land} is the unit price of land ($/$m^2$), x_{upper}, x_{lower}, y_{upper}, and y_{lower} are the upper and lower boundaries in the x-axis and y-axis of the park (m), and n_{plant} is the number of plants in the industrial park. It should be noticed that there is also a distance of d/2 between plants and the boundary of the industrial park.

Additionally, the industrial park must be constructed within a specific area and cannot be infinitely large. Therefore, plant coordinates should be limited by the following constraints:

$$x_i + \frac{L_{x,i}}{2} + \frac{d}{2} \le x_{upper,bound} \quad i = 1,2,3.....n_{plant} \tag{14}$$

$$x_i - \frac{L_{x,i}}{2} - \frac{d}{2} \ge x_{lower,bound} \quad i = 1,2,3.....n_{plant} \tag{15}$$

$$y_i + \frac{L_{y,i}}{2} + \frac{d}{2} \le y_{upper,bound} \quad i = 1,2,3.....n_{plant} \tag{16}$$

$$y_i - \frac{L_{y,i}}{2} - \frac{d}{2} \ge y_{lower,bound} \quad i = 1,2,3.....n_{plant} \tag{17}$$

Here, $x_{upper,bound}$, $x_{lower,bound}$, $y_{upper,bound}$, and $y_{lower,bound}$ are the boundaries of the available space where the industrial park can be accommodated.

3.5 Pipe network cost

The pipe network is a kind of special system featured with multiple branches, existing widely in industrial parks. The improved FLUTE algorithm[17] is employed in this work to generate the most economical routing for a pipe network. For example, some plants in an industrial park and their demand for steam are shown in Fig. 1 (a). A negative value means the plant produces steam. The most economical pipe network interconnecting all plants can be obtained by the improved FLUTE algorithm, as shown in Fig. 1 (b). The arrows indicate the flow directions and the thickness of a line indicates the diameter of the pipe.

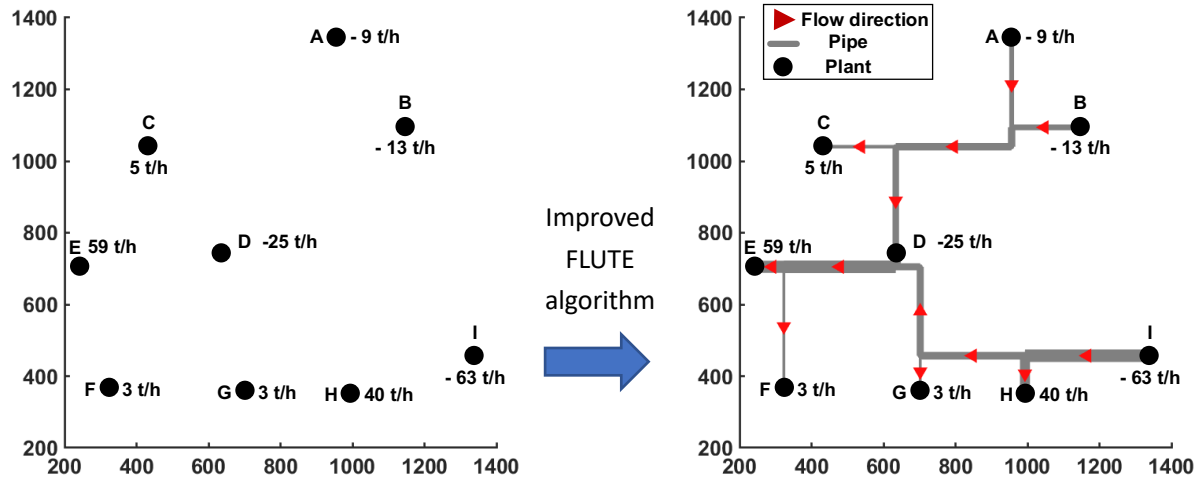

(a) Location and steam demand of plants (b) The most economical pipe network

Fig. 1. Illustration of the improved FLUTE algorithm

In graph theory, the problem of constructing a network of minimum length interconnecting a given set of points in the Euclidean plane, where each edge of the network is composed of horizontal and vertical line segments, is known as the Rectilinear Steiner Minimum Tree (RSMT) problem[36]. However, if the flow velocity of materials in a pipe network is given, the diameters of pipe segments in the network will vary due to the different mass flow rates. The unit price will also be different. Therefore, the arrangement problem of the most economical pipe network is considerably more complicated than the basic RSMT problem.

In the improved FLUTE algorithm, the pipe network arrangement problem is simplified to a problem similar to the RSMT problem, and a database with all potentially optimal connections is used. When the locations and consumption/production of plant nodes are given, the algorithm will search in the database for potentially optimal connections. By evaluating and comparing these connection schemes, the most economical connection can be found. More details about the improved FLUTE algorithm can be found in references[15, 17, 37].

The pipe network cost refers to the purchase cost of pipes for pipe networks. Therefore, the pipe network cost can be obtained by Eq. (18).

$$C_{network} = \sum_{j=1}^{n_{network}} \sum_{h=1}^{n_{segment,j}} U_{network,j,h} \times L_{network,j,h} \tag{18}$$

Here, $U_{network,j,h}$ and $L_{network,j,h}$ are the unit price ($) and length (m) of pipe segment h in pipe network j, $n_{segment,j}$ is the number of pipe segments in pipe network j, and $n_{network}$ is the number of pipe networks in the industrial park. The structure of pipe network (including $L_{network,j,h}$, and $n_{segment,j}$) can be obtained from the improved FLUTE algorithm.

3.6 Simple pipe cost

A simple pipe only has one inlet plant and one outlet plant. It transfers materials between the two plants and the cost is easy to calculate according to Eqs. (19) and (20).

$$C_{simple} = \sum_{k=1}^{n_{simple}} U_{simple,k} \times L_{simple,k} \tag{19}$$

$$L_{simple,k} = \left|x_i - x_{i'}\right| + \left|y_i - y_{i'}\right| \tag{20}$$

Here, $U_{simple,k}$ and $L_{simple,k}$ are the unit price ($/m) and length (m) of the simple pipe k, n_{simple} is the number of simple connections, x_i, $x_{i'}$, y_i, and $y_{i'}$ are the coordinates of inlet and outlet plants connected by the simple pipe k (m).

3.7 Expected property loss

Similar to the expected annual fatalities, the expected property loss can be obtained from Eq. (21).

$$C_{property} = T_{life} \sum_{i=1}^{n_{plant}} P_{damage,i} U_{plant,i} \tag{21}$$

Here, $P_{damage,i}$ is the probability of structural damage of plant i (/yr), $U_{plant,i}$ is the purchase cost of plant i ($), and T_{life} is the lifetime of the industrial park (yr).

In most of the previous works, the probabilities of death and structural damage in the center point of a plant are considered as the probabilities for the whole plant. However, the overpressure varies even within the same plant. In this work, the probabilities of death and structural damage are integrated in the domain of the affected plant to obtain the corresponding probabilities for the whole plant, which can be expressed by Eqs. (22) and (23).

$$P_{death,i} = \iint_{Dom_i} P(x,y)_{composite,death} dxdy \quad Dom_i = \left\{(x,y) \mid x_{lower,i} < x < x_{upper,i}, y_{lower,i} < y < y_{upper,i}\right\} \tag{22}$$

$$P_{damage,i} = \iint_{Dom_i} P(x,y)_{composite,damage} dxdy \quad Dom_i = \left\{(x,y) \mid x_{lower,i} < x < x_{upper,i}, y_{lower,i} < y < y_{upper,i}\right\} \tag{23}$$

Here, $P(x,y)_{composite,death}$ and $P(x,y)_{composite,damage}$ are the probabilities of death and structural damage (/yr) in point (x,y), which can be obtained from a composite risk map, Dom_i is the domain of plant i, $x_{lower,i}$, $x_{upper,i}$, $y_{lower,i}$, and $y_{upper,i}$ are the upper and lower bounds of plant i.

3.8 Solution algorithm

In this work, NSGA-II is applied to find the Pareto front. NSGA-II is similar to the classical single-objective GA[31], but significantly different in the step of selection. The principles of NSGA-II will be briefly explained here for a better understanding of the solving process, and this is also helpful in explaining why NSGA-II is used to solve the proposed model and understanding the comparison among NSGA-II, MOPSO, and DMS.

Some concepts should be explained first. A double-objective minimization problem is taken as an example in the following.

Dominance: If both of the two objective values of Solution A are lower than Solution B, it is said that Solution A dominates Solution B, as shown in Fig. 2 (a). In Fig. 2 (b), none of the solutions dominates the other.

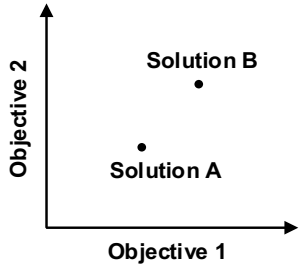

(a) Illustration of dominance

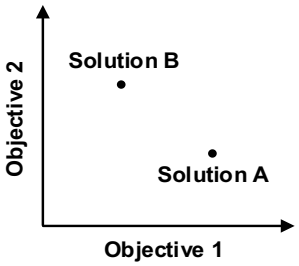

(b) No one dominates the other

Fig. 2. Illustration of dominance

Rank: If the highest rank among all the solutions that dominate Solution C is R, then the rank of Solution C is R+1. This concept is illustrated in Fig. 3. Therefore, solutions with a lower rank are better. Solutions in the Pareto front are not dominated by any other solutions and have rank = 1.

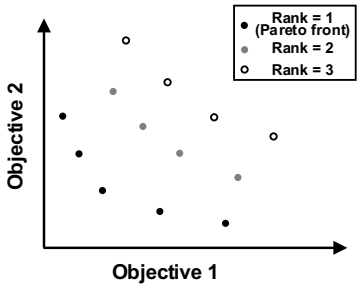

Fig. 3. Illustration of rank

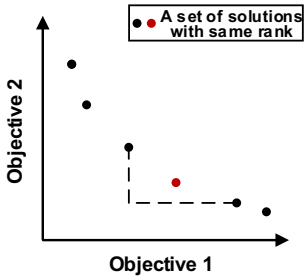

Fig. 4. Illustration of distance

Distance: A distance indicates the closeness of a solution to its nearest neighbors with the same rank. The distance of a solution is equal to the sum of differences between the objective function values of the two nearest solutions. The length of the dashed line is the distance of the red point, as shown in Fig. 4. The distance of solutions at the extreme positions is set to infinite. Distance is used to measure the variety of a solution. For solutions with the same ranks, the solution with a higher distance is better.

Therefore, the solving process of NSGA-II can be briefly described as follows: A set of solutions known as the first generation is developed randomly and evaluated to obtain objective function values. Solutions are called individuals in NSGA-II. The individuals are sorted according to their ranks. Individuals with the same rank are sorted according to their distance. The selection, crossover, and mutation operators are implemented to keep the best individuals and reproduce a new generation. This is repeated until a pre-set number of generations is reached. The curve composed by the individuals with rank = 1 is considered to be the final Pareto front.

In this work, the death penalty function is employed to deal with constraints. Each individual will be checked whether it is feasible or not according to constraints before being evaluated by the proposed model. If it is infeasible, the two objectives of the individual are assigned very large values. If it is feasible, the individual is evaluated according to the model.

The complete flow diagram of the solving process is shown in Fig. 5.

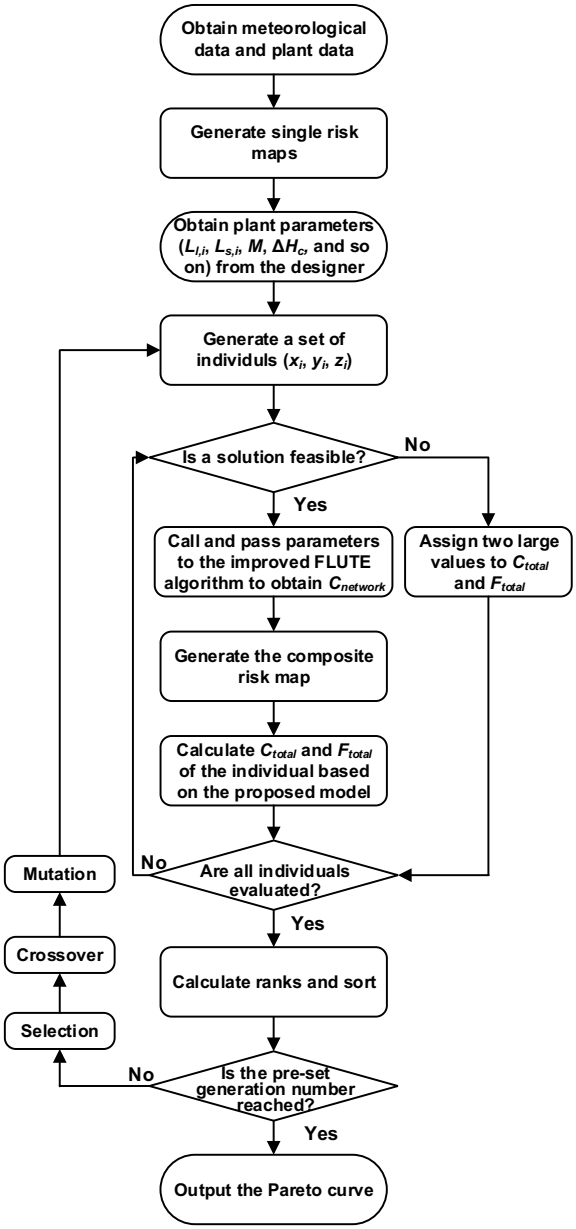

Fig. 5. Complete flow diagram of the solving process

4 Generation of the composite risk map

In Section 3, all the parameters are known except $P(x,y)_{composite,death}$ and $P(x,y)_{composite,damage}$, which can be obtained from a composite risk map. A composite risk map records the death probability (or structural damage probability) in every point of the industrial park under a specific layout considering all hazard sources. The meteorological condition, which is highly uncertain, determines the distribution of toxic gas and the death probabilities in the industrial park when a toxic release accident occurs. Vázquez-Román et al.[25] proposed a method to generate a risk map based on historical meteorological data. In this work, their method is improved and extended to generate a composite risk map. For a better understanding of the extended risk map method, their approach is briefly explained here.

4.1 The risk map method by Vázquez-Román et al.

The historical meteorological data, including wind speed, wind direction, and atmospheric stability per hour from several years, are needed to draw a risk map. The procedure is:

(1) Count the number of values of wind speed, wind direction, and atmospheric stability respectively, and fit the statistics by formulas with specific forms to obtain three probability density functions (PDFs).
(2) Randomly generate a wind speed, wind direction, and atmospheric stability based on the PDFs independently and combine them into one meteorological scenario.
(3) Employ an appropriate diffusion model to calculate the distribution of toxic gas under the obtained meteorological scenario.
(4) Repeat steps (2) - (3) a very large number of times (e.g. 10,000) to obtain the distributions. Calculate the average concentration of toxic gas in every point of the industrial park.
(5) Calculate the corresponding death probability based on the concentration at every point. In fact, a risk map has been obtained in this step.
(6) Fit the death probabilities by a formula with a specific form (risk equation).

When the coordinates of a point are given, the corresponding death probability can be obtained by the risk equation. The risk equation is then integrated into the objective function to provide death probabilities of toxic release. The procedure above is executed only once for a certain case.

4.2 Extended risk map method

The original method synthesizes the historical meteorological data to consider the uncertainty of meteorological conditions. However, only toxic release accidents were considered. In addition, the original method has four inherent disadvantages:

(a) Fittings with certain forms are implemented several times in the process, which will introduce significant deviation compared with the original data.

(b) Three meteorological parameters are generated independently in step (2), however, wind speed and atmospheric stability are related. Table 1 shows the definition of atmospheric stability. The atmospheric stability is determined by wind speed and solar radiation. When the wind speed is 3-5 m/s, the atmospheric stability can only be B or C. However, in the original method, it is entirely possible to generate invalid data like “4 m/s, D”.

(c) High wind speed may typically occur in a certain direction, rather than happen in all directions with the same probability.

(d) The average death probabilities rather than the average of concentrations should be calculated. A death probability based on the average concentration will not be representative for the actual situation.

Table 1 Definition of atmospheric stability [38]

Wind speed	Daytime solar radiation			Nighttime cloud cover	
m/s	Strong	Moderate	Slight	>50%	<50%
<2	A	A-B	B	E	F
2-3	A-B	B	C	E	F
3-5	B	B-C	C	D	E
5-6	C	C-D	D	D	D
>6	C	D	D	D	D

Therefore, an extended risk map method is proposed in this work to overcome the disadvantages of the original method. The extended risk map method generates a composite risk map by integrating the single risk maps of all hazard sources. A single risk map indicates the distribution of death probability (or structural damage probability) when an accident occurs in the hazard source. Mathematically, the probability of death and structural damage probability at a certain point in the composite risk map can be obtained by Eqs. (24) and (25).

$$P(x,y)_{composite,death} = \sum_{m=1}^{n_{hazard}} P(x,y)_{death,m} P_{accident,m} \tag{24}$$

$$P(x,y)_{composite,damage} = \sum_{m=1}^{n_{hazard}} P(x,y)_{damage,m} P_{accident,m} \tag{25}$$

Here, $P(x,y)_{death,m}$ and $P(x,y)_{damage,m}$ are the probabilities of death and structural damage in point *(x,y)* when an accident occurs in hazard source *m*, which can be obtained from single risk maps, and $P_{accident,m}$ is the probability of accident (/yr) of hazard source *m*.

In other words, single risk maps show the death probabilities when an accident occurs, while a composite risk map considers the chances of accidents. Besides, since the safety of workers is emphasized in this work, the term "single/composite risk map" in the following refers to the single/composite risk map with death probabilities for people, rather than those with structural damage probabilities.

The generation procedure of a single risk map is different for different types of hazard sources. In this work, two types of common accidents, explosion and toxic release, are considered. It is worth mentioning that the proposed extended risk map method is still extendable and flexible. Various types of accidents can be included in the proposed framework, and other evaluation methods can also be used.

4.2.1 Generation of single risk map for toxic release sources

The generation of a single risk map for the plant with a potential toxic release is based on the method by Vázquez-Román et al.[25] with a significant improvement. The data for wind speed, wind direction, and atmospheric stability from the same original record of meteorological data are used to generate the distribution scenarios, and the average death probabilities are then calculated. The procedure is:

(1) Randomly select a piece of record from the meteorological data with simultaneous values for wind speed, wind direction, and atmospheric stability.

(2) Calculate the concentration in every point of the industrial park based on a Pasquill-Gifford model which is expressed by Eq. (26) [39].

$$C(x,y,h) = \frac{Q}{2\pi\sigma_y\sigma_h u}\exp\left[-\frac{1}{2}\left(\frac{y}{\sigma_y}\right)^2\right]\times\left\{\exp\left[-\frac{1}{2}\left(\frac{h-H}{\sigma_h}\right)^2\right]+\exp\left[-\frac{1}{2}\left(\frac{h+H}{\sigma_h}\right)^2\right]\right\} \tag{26}$$

Here, *C* is the concentration of toxic gas in the receptor point (kg/m^3), *x, y,* and *h* are the coordinates and height of a receptor point (m), *Q* is the release rate (kg/s), *H* is the height of the release point (m), σ_y and σ_h are the dispersion coefficients, which can be obtained from Table 2.

(3) Calculate the corresponding death probability at every point based on the concentration. The relationship between concentration and death probability is different for different toxic gases and can be found in reference[40].

Table 2 Dispersion coefficients of the Pasquill-Gifford model

Atmospheric stability	Dispersion coefficients		
	σ_y	σ_h	
A	$\sigma_y=0.493x^{0.88}$	$\sigma_h=0.087x^{1.10}$	$100 < x < 300$
		$\log_{10}\sigma_h= -1.67 + 0.902\log_{10} x + 0.181(\log_{10} x)^2$	$300 < x < 3000$
B	$\sigma_y=0.337x^{0.88}$	$\sigma_h=0.135x^{0.95}$	$100 < x < 500$
		$\log_{10}\sigma_h= -1.25 + 1.09\log_{10} x + 0.0018(\log_{10} x)^2$	$500 < x < 2\times10^4$
C	$\sigma_y=0.195x^{0.90}$	$\sigma_h=0.112x^{0.91}$	$100 < x < 10^5$
D	$\sigma_y=0.128x^{0.90}$	$\sigma_h=0.093x^{0.85}$	$100 < x < 500$
		$\log_{10}\sigma_h= -1.22 + 1.08\log_{10} x - 0.061(\log_{10} x)^2$	$500 < x < 10^5$
E	$\sigma_y=0.091x^{0.91}$	$\sigma_h=0.082x^{0.82}$	$100 < x < 500$
		$\log_{10}\sigma_h= -1.19 + 1.04\log_{10} x - 0.070(\log_{10} x)^2$	$500 < x < 10^5$
F	$\sigma_y=0.067x^{0.90}$	$\sigma_h=0.057x^{0.80}$	$100 < x < 500$
		$\log_{10}\sigma_h= -1.91 + 1.37\log_{10} x - 0.119(\log_{10} x)^2$	$500 < x < 10^5$

(4) Repeat steps (1) - (3) a very large number of times to obtain distributions of death probability. Calculate the average death probabilities to obtain a single risk map.

For each potential release plant, the steps above are executed once. Therefore, if there are several plants with potential toxic release, several single risk maps will be obtained. In the improved method, the original data are used in sets to avoid fitting and ensure the validity of each set of data.

4.2.2 Generation of single risk maps for explosive sources

The TNT equivalent model is an effective method to estimate the intensity of an explosion. It is used here to find the distribution of overpressure when an explosion accident occurs. The probability of death for people and structural damage for buildings can be obtained according to the overpressure.

The TNT equivalent model is described by Eqs. (27) - (30) [40].

$$M_{TNT}=\alpha\frac{M\Delta H_c}{E_{TNT}} \tag{27}$$

$$z_{TNT}=\frac{R}{M_{TNT}^{\frac{1}{3}}} \tag{28}$$

$$B_{TNT}=\mathrm{a_{TNT}}+\mathrm{b_{TNT}}\log_{10} z_{TNT} \tag{29}$$

$$\log_{10} p^0=\sum_{r=0}^{11} c_r B_{TNT}{}^r \tag{30}$$

Here, M is the mass of explosive material in the plant (kg), E_{TNT} is the explosion energy of TNT which is 4190-4650 kJ/kg, ΔH_c is the combustion heat of explosive material (kJ/kg), M_{TNT} is the equivalent mass of TNT (kg), α is a yield factor with value 0.03-0.04, R is the distance between the receptor point and explosion center (m), z_{TNT} is a scaled distance (m/kg$^{1/3}$), a_{TNT}, b_{TNT}, and c_r are constant parameters that are shown in Table 3, B_{TNT} is an intermediate parameter, and P^0 is the peak overpressure in the receptor point (kPa).

With overpressure, the probits of death for a person and structural damage for a building in the receptor point can be calculated by Eqs. (31) [40] and (32) [40].

Table 3 Parameters of the TNT equivalent model

Parameter	Value	Parameter	Value
a_{TNT}	-0.21436	b_{TNT}	1.35034
c_0	2.78077	c_1	-1.69590
c_2	-0.15416	c_3	0.51406
c_4	0.09885	c_5	-0.29391
c_6	-0.02681	c_7	0.10910
c_8	0.00163	c_9	-0.02146
c_{10}	0.00015	c_{11}	0.00168

$$Y_{explosion,death} = -77.1 + 6.91 \ln p^0 \tag{31}$$

$$Y_{explosion,damage} = -23.8 + 2.92 \ln p^0 \tag{32}$$

Here, $Y_{explosion,death}$ is the probit of death and $Y_{explosion,damage}$ is the probit of structural damage.
The probit can then be converted to probability according to Eq. (33).

$$P=50\left[1+\frac{Y\text{-}5}{|Y\text{-}5|}\operatorname{erf}\left(\frac{Y-5}{\sqrt{2}}\right)\right] \tag{33}$$

Here, Y is the probit, P is the corresponding probability, and erf is error function.
Therefore, the distribution of death probability and the single risk map for an explosive source can be obtained. A composite risk map can be generated by integrating the single risk maps of all hazard sources.

5 Case study

Two cases are demonstrated in this Section. The first case study is from Vázquez-Román et al. [25] so that the results can be used to illustrate the advantages of the proposed method compared with traditional layout optimization methods with single-objective. The second case study is much larger and more complicated than the first one in order to demonstrate all the features of the proposed method.

5.1 Case 1: Moderate size industrial park

This case discussed by Vázquez-Román et al.[25] involves an industrial park with five plants, two of which have been allocated their locations. Thus, only three plants are left for location determination. The dimensions of the plants are shown in Table 4, and the coordinates of the two fixed plants are shown in Table 5. Plants NA-FA and NA-NB are connected by two simple pipes. The pipe price is 98.4 \$/m. The land price is 6 \$/m^2. CR is a control room with 10 people. Plant FA has a potential chlorine release with a height of 1 m, a rate of 3.0 kg/s, and a frequency of 5.8×10^{-4} /yr. The height of the receptor point is 1.7 m, which is same as the standard height of a human. The minimum distance between plants for roads is 5 m. The presence of pipe networks and possible explosion accidents are not considered in this case. The meteorological data of Corpus Christi from 1981-1990 are used. All the parameters and data are taken from Vázquez-Román et al.[25]. The boundary of the free space is 0-80 m for both x-axis and y-axis.

Table 4 Plant dimensions of Case 1

Plant name	Length of long edge $L_{l,i}$ (m)	Length of short edge $L_{s,i}$ (m)
FA	20	10
FB	15	15
NA	30	10
NB	30	15
CR	15	15

Table 5 Coordinates of fixed plants in Case 1

Plant name	x-axis	y-axis
FA	12.5	7.5
FB	10	25

The probit of death from chlorine, $Y_{Cl2,death}$, can be obtained from Eq. (34) as a function of concentration, C, and exposure time, T_{expo}. In this case T_{expo} = 10 min.

$$Y_{Cl_2,death} = -8.29 + 0.92\ln(C^2 T_{expo}) \tag{34}$$

The extended risk map method is implemented to obtain the risk map. The data are selected 10,000 times. The shapes of the single risk map and the composite risk map are the same for this case because only one hazard source is considered. Therefore, only the single risk map is shown in Fig. 6, in which the center point of (0,0) is the location of the toxic plant FA.

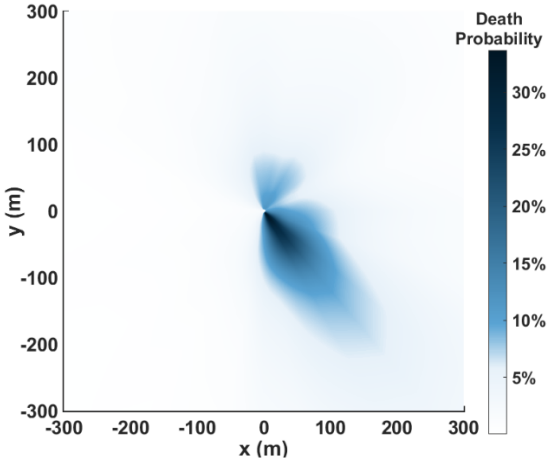

Fig. 6. The single risk map of Case 1

The proposed layout design method is implemented for this case, and NSGA-II is applied to solve the model. The program was run on a MATLAB platform at a workstation with two Xeon E5620 CPUs and Windows 10 operating system. The population size and number of generations are set to be 4,000 and 1,000, respectively. It took 17 minutes to obtain the results. The time for risk map generation is not accounted for.

The Pareto curve obtained is shown in Fig. 7 with pentagram points. Each point represents a solution for the layout. The obtained Pareto curve is composed of 15 points. Due to space limitations, we cannot show all the 15 layouts. The 1st, 5th, 8th, 12th, and 15th solutions are included in Fig. 7, which illustrates the gradual change of layout from "economical" to "safe". The numerical results are shown in Table 6.

In the work by Vázquez-Román et al.[25], the objective function is composed of land cost, simple pipe cost, and risk cost. The risk cost is equal to the compensation multiplied by the expected fatalities. Three solvers based on GAMS were applied to the case, and two different layouts were obtained. It is worth mentioning that for this case, the economic cost models in the objective function are the same for the method by Vázquez-Román et al.[25] and our method. Constraints are also the same. Therefore, the results from the two

methods are completely comparable, i.e. for the same layout, the economic objective function will have the same value.

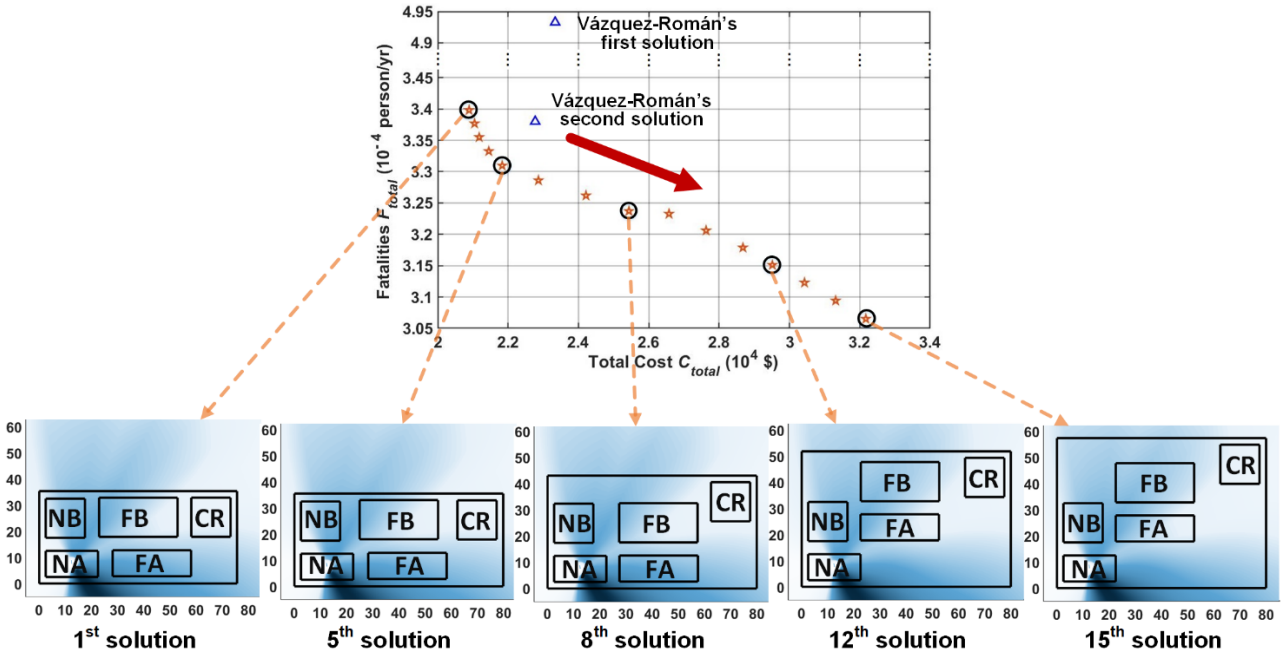

Fig. 7. Pareto curve and some solutions of Case 1

The two solutions from the work by Vázquez-Román et al.[25] are evaluated by the proposed model to obtain the safety performance, and certainly, the costs obtained from our method are the same as those reported by Vázquez-Román et al. The results are marked in Fig. 7 with triangle points. The corresponding layout diagrams and numerical results are shown in Fig. 8 (a), (b), and Table 6.

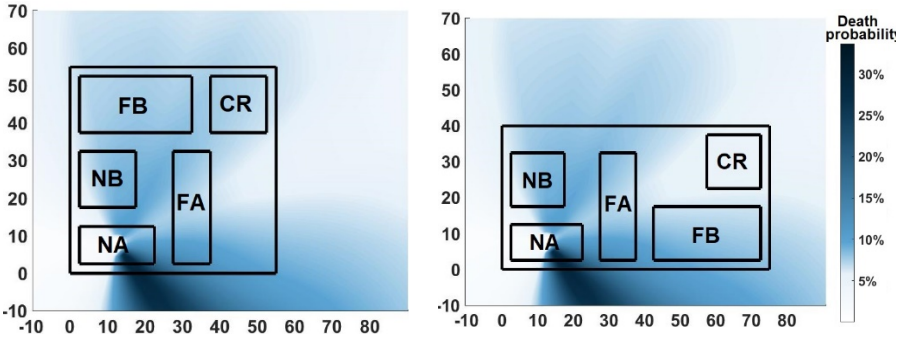

(a) Layout of the first solution from Vázquez-Román et al.

(b) Layout of the second solution from Vázquez-Román et al.

Fig. 8. Layout diagrams of Case 1 from Vázquez-Román et al.

Table 6 Numerical results of Case 1

	Land cost C_{land} ($)	Pipe cost C_{simple} ($)	Total capital cost C_{total} ($)	Expected annual fatalities F_{total} (10^{-4} person/yr)
1st solution from the proposed method	16,070	4,819	20,889	3.40
5th solution from the proposed method	17,032	4,799	21,831	3,31
8th solution from the proposed method	20,757	4,677	25,434	3.24
12th solution from the proposed method	24,908	4,605	29,514	3,15
15th solution from the proposed method	27,562	4,607	32,170	3,06
1st solution by Vázquez-Román et al.	18,150	5,282	23,432	4.93
2nd solution by Vázquez-Román et al.	18,000	4,769	22,769	3.38

In Fig. 7, a set of solutions achieving different trade-offs between economy and safety is obtained from the proposed method. From the 1st solution to the 15th solution, the area of the park increases gradually, while the control room, where 10 people are working, is placed farther away from the toxic plant FA. The park becomes gradually safer, and also more expensive. The designer can therefore make a decision based on the Pareto curve and the actual situation and is free to balance economy and safety. On the contrary, the traditional method only provides one solution, and a decision maker has no choice but to accept.

The 2nd solution from Vázquez-Román et al. is close to the top left of the Pareto curve in Fig. 7. It means that this solution tends to be more economical but with higher risk, and the pre-set compensation in Vázquez-Román et al. (10,000,000 $/death) is relatively low. If the compensation is increased, it can be deduced that the point from Vázquez-Román et al. will shift along the Pareto curve, as the red arrow indicates in Fig. 7. In the proposed method, no compensation is involved, and the ethical problem of measuring human life with money is avoided.

5.2 Case 2: A comprehensive case

This case comes from a real chlor-alkali plant with polyvinyl chloride (PVC) production and contains 13 plants, two of which have been given a location. Three levels of steam pipe networks, high-pressure, medium-pressure, and low-pressure, are considered. Detailed information on the three levels of steam is shown in Table 7. Sch 80 pipes are used in steam pipe networks, while both Sch 40 and Sch 80 pipes are used for simple pipe connections. The information on plants, including dimensions, demands for steam, number of workers, and costs, are shown in Table 8. For steam demands in Table 8, a negative value means the plant produces steam. 42 single connections (material flows) are also considered, as shown in Table 9. The flow velocity is 1 m/s for liquid and 10 m/s for gas[41]. Plants 2 and 8 have a potential chlorine (Cl_2) and hydrogen chloride (HCl) release, respectively, with a height (H) of 1 m and a rate (Q) of 3 kg/s. The height of a receptor point (z_h) is 1.7 m. The probabilities of explosion[40] and toxic release[25] accidents are 1.4×10^{-4} /yr and 5.8×10^{-4} /yr. Plants 3 and 4 are potentially explosive with 1 ton hydrogen and 20 ton acetylene (M). The combustion heats (ΔH_c) are 1.41×10^5 kJ/kg and 5×10^4 kJ/kg, respectively. The energy of TNT explosion (E_{TNT}) and the yield factor (α) are set to 4200 kJ/kg and 0.04, respectively. The meteorological data of Corpus Christi from 1981-1990 are also used for this case.

The probit of death from hydrogen chloride is expressed by Eq. (35) [40]. In this case, T_{expo} = 10 min. The probit of death from chlorine is shown in Eq. (34).

$$Y_{HCl,death} = -16.85 + 2\ln(CT_{expo}) \tag{35}$$

Here, $Y_{HCl,death}$ is the probit of death from hydrogen chloride.

Table 7 Information on the three levels of steam in Case 2

Steam level	Temperature T_{st} (℃)	Pressure p_{st} (MPa)	Density ρ_{st} (kg/m^3)	Velocity v_{st} (m/s)
High-pressure steam	450	4.8	15.463	45
Medium-pressure steam	240	1.6	7.723	35
Low-pressure steam	159	0.5	3.175	25

Table 8 Information on plants in Case 2

Plant No.	Length of long edge $L_{l,i}$ (m)	Length of short edge $L_{s,i}$ (m)	High-pressure steam demand (t/h)	Middle-pressure steam demand (t/h)	Low-pressure steam demand (t/h)	Number of workers N_{worker}	Cost $U_{plant\ i}$ (10^3 \$)
1	27	16	0	0	10	2	300
2	30	13	0	0	0	2	170
3	31	28	5	0	30	2	500
4	45	28	0	7	0	0	520
5	31	16	0	0	5	20	250
6	40	15	20	0	9	0	320
7	29	27	-112	-142	-75	2	400
8	31	31	0	18	-30	0	330
9	28	21	0	42	14	4	280
10	38	20	21	15	24	2	460
11	29	26	30	8	13	0	460
12	23	11	24	20	0	2	340
13	16	16	12	32	0	2	320

Table 9 Data for the simple connections

Flow No.	Output from	Input to	Flow rate q (kg/s)	Density ρ (kg/m^3)	Pipe type
1	6	3	7.50	1000	Sch 40
2	3	8	0.02	0.15752	Sch 80
3	3	8	0.52	5.6	Sch 80
4	3	9	0.71	1000	Sch 40
5	3	2	0.14	5.6	Sch 80
6	8	10	0.49	1.98	Sch 80
7	4	10	0.31	1.446	Sch 80
8	10	11	0.66	923	Sch 80
9	11	10	0.00	923	Sch 80
10	11	2	0.75	923	Sch 80
11	7	11	0.56	8.9	Sch 80
12	7	9	0.89	8.9	Sch 80
13	7	13	0.21	8.9	Sch 80
14	7	5	0.07	8.9	Sch 80
15	13	10	33.33	1000	Sch 40
16	13	5	2.78	1000	Sch 40
17	12	11	16.67	1000	Sch 40
18	11	12	16.67	1000	Sch 40
19	12	10	12.78	1000	Sch 40
20	10	12	12.78	1000	Sch 40
21	12	3	13.89	1000	Sch 40
22	3	12	13.89	1000	Sch 40
23	3	6	7.50	1000	Sch 40
24	13	6	0.31	6.78	Sch 40

25	13	3	0.35	6.78	Sch 40
26	13	11	0.45	6.78	Sch 40
27	13	12	33.33	1000	Sch 40
28	12	8	16.67	1000	Sch 40
29	12	8	16.67	1000	Sch 40
30	8	2	0.05	1.98	Sch 80
31	13	4	0.45	6.78	Sch 40
32	13	4	33.33	1000	Sch 40
33	13	4	33.33	1000	Sch 40
34	13	4	22.22	1000	Sch 40
35	13	4	22.22	1000	Sch 40
36	4	2	11.11	1000	Sch 40
37	2	11	2.78	1050	Sch 40
38	2	11	1.78	1200	Sch 40
39	2	11	0.89	900	Sch 40
40	2	11	1.50	1210	Sch 40
41	2	11	2.33	950	Sch 40
42	2	11	2.39	970	Sch 40

For both simple pipes and pipe networks, the unit price of a pipe is obtained from Eqs. (36) - (43) [42].
For Sch 40 pipes:

$$D_{inner} = \sqrt{\frac{4q}{\pi \rho v}} \tag{36}$$

$$D_{outer} = 1.052 D_{inner} + 0.005251 \tag{37}$$

$$wt_{pipe} = 644.3 D_{inner}^2 + 72.5 D_{inner} + 0.4611 \tag{38}$$

$$U_{pipe} = E_1 wt_{pipe} + E_2 D_{outer}^{0.48} + E_3 + E_4 D_{outer} \tag{39}$$

For Sch 80 pipes:

$$D_{inner} = \sqrt{\frac{4q}{\pi \rho v}} \tag{40}$$

$$D_{outer} = 1.101 D_{inner} + 0.006349 \tag{41}$$

$$wt_{pipe} = 1330 D_{inner}^2 + 75.18 D_{inner} + 0.9268 \tag{42}$$

$$U_{pipe} = \mathrm{E}_1 wt_{pipe} + \mathrm{E}_2 D_{outer}^{0.48} + \mathrm{E}_3 + \mathrm{E}_4 D_{outer} \tag{43}$$

Here, U_{pipe} is the unit price of a pipe ($/m), E_1-E_4 are constant parameters with the values of 0.82, 185, 6.8, and 295, respectively, wt_{pipe} is the pipe weight per unit length (kg/m), D_{inner} and D_{outer} are the inner and outer diameters (m).
The program was run on the same machine as in Case 1. The obtained Pareto curve is shown in Fig. 9. The single risk maps are shown in Fig. 10 (a) - (d). The median solution is drawn as an example. The composite

risk map, steam pipe networks, and numerical results of the median solution are shown in Fig. 10 (e), Fig. 11 and Table 10.

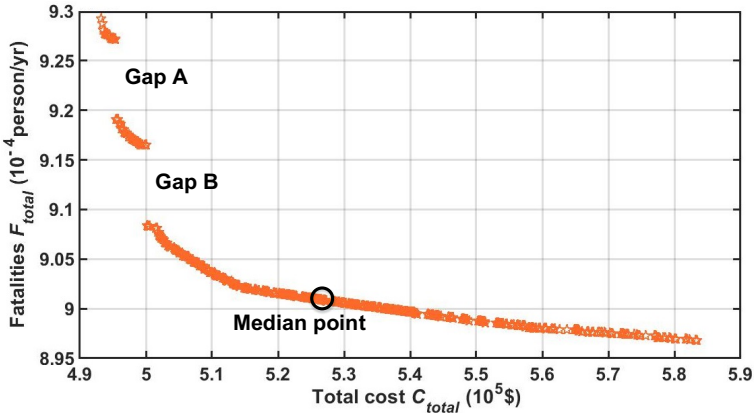

Fig. 9. Pareto curve of Case 2

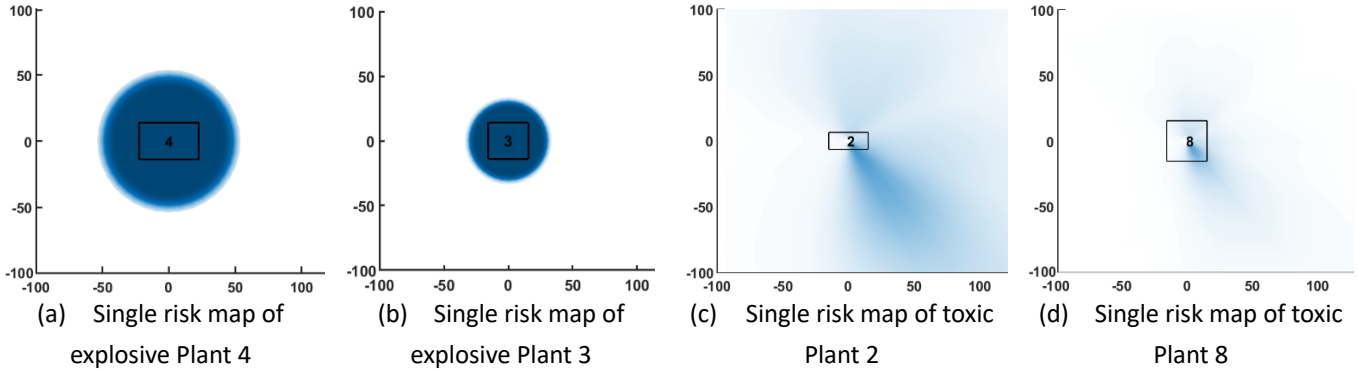

(a) Single risk map of explosive Plant 4 (b) Single risk map of explosive Plant 3 (c) Single risk map of toxic Plant 2 (d) Single risk map of toxic Plant 8

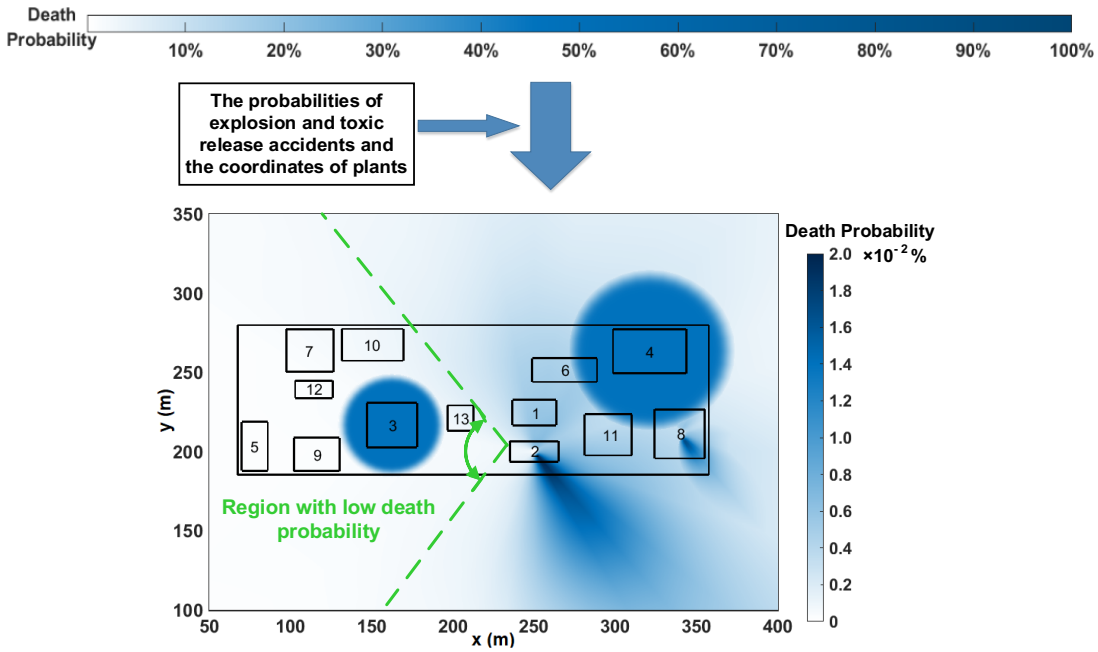

(e) The composite risk map of the median solution

Fig. 10. Single risk maps and the composite risk map of the median solution for Case 2

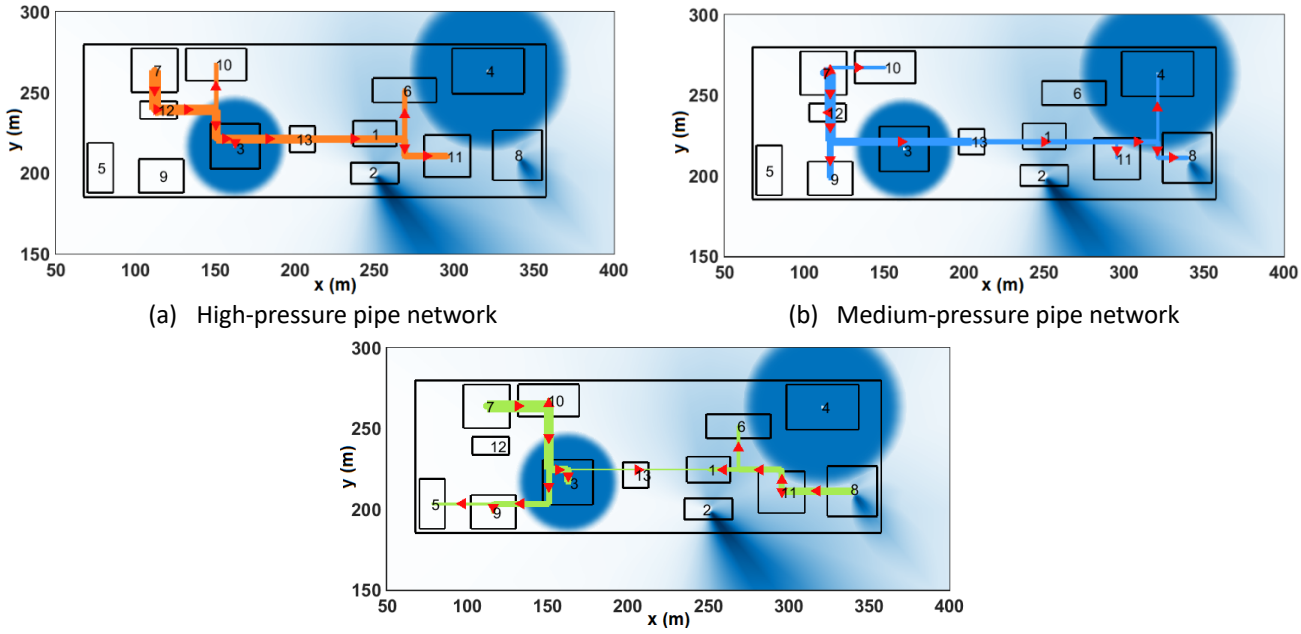

(a) High-pressure pipe network

(b) Medium-pressure pipe network

(c) Low-pressure pipe network

Fig. 11. Pipe networks of the median solution for Case 2

Table 10 Numerical results of the median solution of Case 2

Objective 1	Value	Objective 2	Value
Total capital cost C_{total} ($)	526,286	Total fatalities F_{total} (10^{-3} person/yr)	0.901
Land cost C_{land} ($)	164,576	Fatalities from explosion $F_{explosion}$ (10^{-3} person/yr)	0.620
Simple pipe cost C_{simple} ($)	26,260	Fatalities from toxic release F_{toxic} (10^{-3} person/yr)	0.281
Pipe network cost $C_{network}$ ($)	292,676		
Expected property loss $C_{property}$ ($)	42,773		

In Fig. 9, the proposed method produces 709 solutions and provides the designer with a high degree of freedom to achieve different trade-offs between economy and safety. It is worth noting that the Pareto curve obtained is discontinuous with 2 large gaps. A significant change of layout may be the reason for the discontinuity of the Pareto curve, which will be discussed in detail in Section 5.2.2.

For Fig. 10, it is worth reminding again that the probabilities in single risk maps are the death probabilities under a deterministic accident, while the probabilities in the composite risk map consider the chances of accidents. Therefore, the probabilities in single risk maps are much higher than those in the composite risk map. The color in Fig. 10 (a) and (b) is darker than that in Fig. 10 (c) and (d), which means the death probabilities of an explosion are higher than those of a toxic release. However, after considering the accident probabilities, in Fig. 10 (e), death probabilities near toxic plants are higher than those near explosive plants. In Fig. 10 (e), apart from the southeastern side of Plant 2, the northern side of Plant 2, where Plants 1 and 6 are located, is also dangerous with considerable death probabilities. A region with sector shape in the west of the available space is relatively safe with low death probabilities, as shown in Fig. 10 (e) with dashed lines. All plants with workers are located in this safe region, while plants without workers (Plants 4, 6, 8 and 11) are located in the east of the available space with high death probabilities. The industrial park has a narrow rectangle shape so that as many plants as possible can be located in the area with low death probability. Plant 5, the control room with a lot of workers, is located farthest from the hazard sources. Also, all plants around the explosive Plant 3 are in good distance from it to ensure their safety. Therefore, the proposed method tries to ensure safety under a certain economic situation.

5.2.1 Details of the trade-off in Pareto curve

709 solutions are obtained in Case 2, which achieve different trade-offs between economy and safety. The total cost, expected fatalities, occupied land area, and pipe steel weight are calculated and plotted in Fig. 12 to explore how these solutions make trade-offs between economy and safety. These solutions are sorted according to their total costs from high to low. According to the principle of NSGA-II, this sequence is also the same as the sequence based on their expected fatalities from low to high.

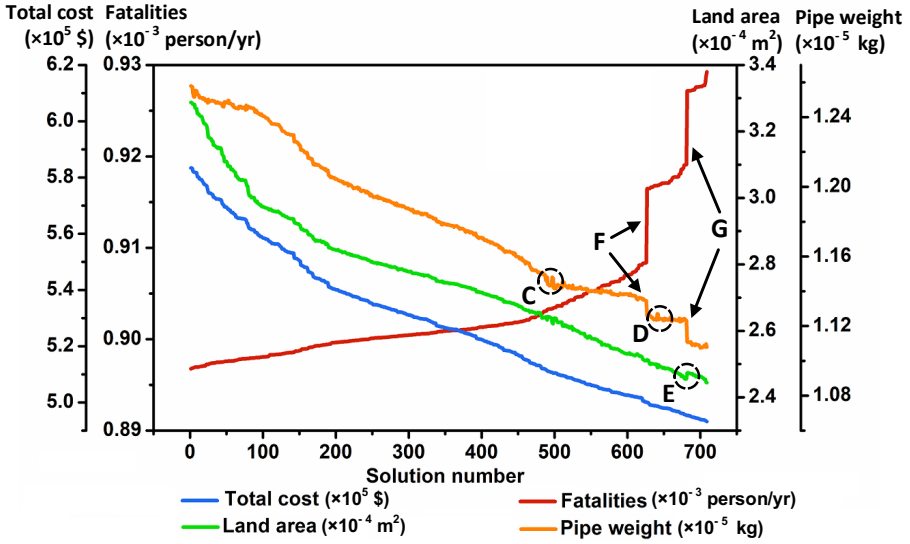

Fig. 12. The total costs, fatalities, land areas, and pipe weights of the 709 solutions in Case 2

In Fig. 12, the total cost is reduced all the way, while the number of fatalities is increased, which agrees with the principle of NSGA-II. For land area and pipe weight, on the whole, they are in decline indicating that the industrial park becomes smaller and smaller from Solution 1 to Solution 709. However, in some points like Points C, D, and E in Fig. 12, the land area and pipe weight are increased. For these solutions, other costs are reduced to counteract the increase of land or pipe cost to maintain a monotonic reduction in total cost. For example, for Point E, the land area is increased, while the pipe consumption is reduced. Therefore, the proposed method tries to balance different factors to achieve different trade-offs between economy and safety.

5.2.2 Discontinuities in the Pareto curve

In Fig. 9, two significant gaps A and B are observed. Interestingly, corresponding to gaps A and B, some gaps also appear in Fig. 12 marked by “F” and “G”. The solutions in “G” (corresponding to gap A) are the 681th and 682th solutions. In this section, Solution 681 and 682 are analyzed to explore what changes were made from Solution 681 to 682 and thereby reason for the discontinuity in the Pareto curve.

The numerical results of Solutions 681 and 682 are shown in Table 11. Solution 682 is more economical with a higher risk. Theoretically, this solution is expected to have a smaller land area, lower pipe cost, and more expected fatalities than Solution 681, however, as shown in Table 11, the situation is more complicated and different from our expectations. Two abnormal phenomena are observed: (a) The more economical Solution 682 has a higher land cost. (b) The more economical Solution 682 also has less expected fatalities from explosions. However, two opposite effects are also observed that make the final values of the two objectives

agree with the theory: for phenomenon (a), the more economical Solution 682 has a much lower pipe cost that counteracts the increase in land cost. For phenomenon (b), the more economical Solution 682 has much higher number of expected fatalities from toxic release, which results in an increase in total number of expected fatalities.

The analysis above describes the compromise among different factors. However, more details need to be investigated to explore how the proposed method achieves these compromises among various factors. The layout and pipe networks for Solutions 681 and 682 are shown in Fig. 13 and Fig. 14.

Table 11 Numerical results of Solutions 681 and 682

Item	Solution 681	Solution 682	Difference
Land cost C_{land} ($)	147,320	148,414	1,093
Simple pipe cost C_{simple} ($)	23,889	23,683	-206
Pipe network cost $C_{network}$ ($)	279,778	278,728	-1,050
Expected property loss $C_{property}$ ($)	44,431	44,547	116
Total cost C_{total} ($)	495,419	495,372	-47
Expected fatalities from toxic release F_{toxic} (10^{-3} person/yr)	0.637	0.646	0.009
Expected fatalities from explosion $F_{explosion}$ (10^{-3} person/yr)	0.282	0.281	-0.001
Total expected fatalities F_{total} (10^{-3} person/yr)	0.919	0.927	0.008
Pipe steel weight (kg)	112,320	111,099	-1,221

From Fig. 13 and Fig. 14, it is observed that the location of Plant 13 is significantly different, which results in significantly different arrangements for high- and medium-pressure steam pipe networks. In addition, Plants 9 and 13 are very close to the affected area of Plant 3 in Solution 681. Plant 13 is placed somewhere with higher death probabilities in Solution 682.

The gaps in Fig. 9 and Fig. 12 can now be understood. From Solution 681 to Solution 682, the total cost is supposed to be reduced. If the layout of Solution 681 is kept, while just contracting the land to construct Solution 682 (called Plan A), Plants 9 and 13 will get into the affected area of Plant 3 and the expected fatalities will increase significantly. Instead, however, the proposed method moves Plant 13 northwards to reconstruct the high- and medium-pressure steam pipe networks in order to reduce the pipe network cost and thereby the total cost. However, Plant 13 is placed somewhere with higher death probabilities, and the number of expected fatalities from toxic releases is considerably increased. The occupied land is then to some extent expanded to increase the distance between plants and mitigate the increase of expected fatalities. Therefore, the land cost is increased, and the number of expected fatalities from explosions is decreased. Finally, from Solution 681 to Solution 682, the total cost is stable with a very small reduction, while the number of expected fatalities is significantly increased (the increase is still less than Plan A) due to the considerable change of layout. All these factors result in the discontinuity of the Pareto curve (Gap A in Fig. 9).

Therefore, industrial FLPs are severely discontinuous both for the Pareto curve and the feasible region. Generally, a continuous curve can be obtained by slowly moving plants to construct solutions with little differences in safety and economy. However, in some situations, a significantly different layout is needed to extend the Pareto curve and achieve a new balance between safety and economy. Another situation that needs a significantly different layout is when plants already touch each other, and therefore cannot get any closer to reduce total cost.

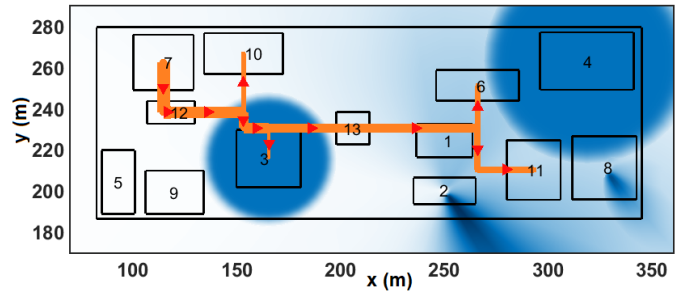

(a) High-pressure steam pipe network

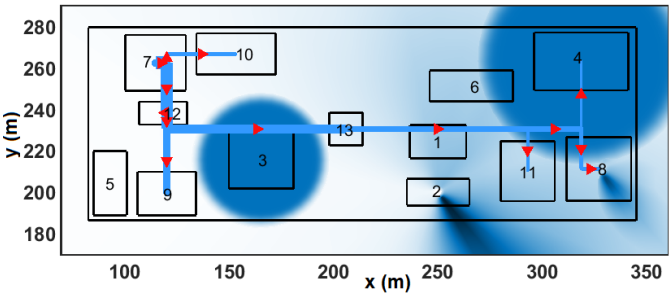

(b) Medium-pressure pipe network

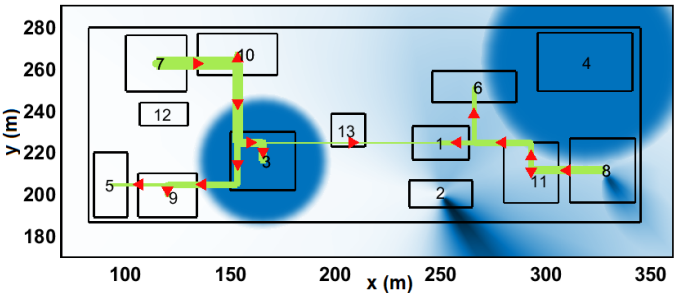

(c) Low-pressure steam pipe network

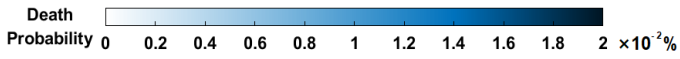

Fig. 13. Pipe networks of Solution 681

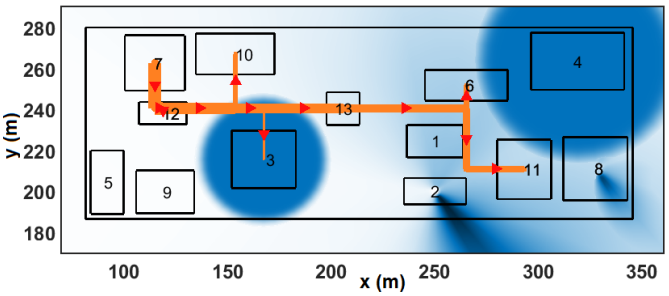

(a) High-pressure steam pipe network

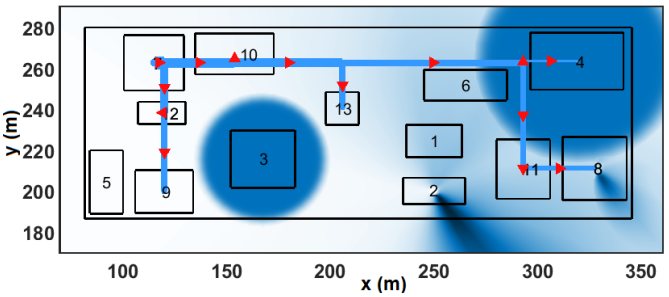

(b) Medium-pressure pipe network

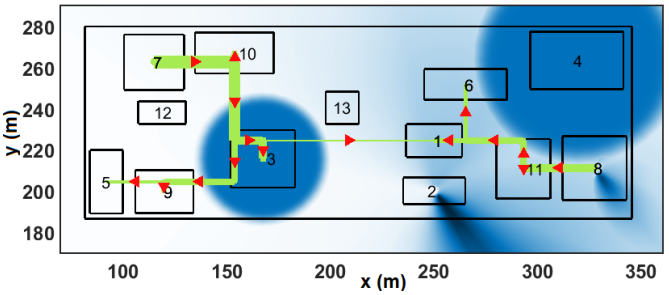

(c) Low-pressure steam pipe network

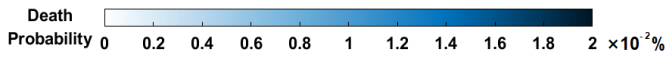

Fig. 14. Pipe networks of Solution 682

However, a significantly different layout does not always lead to a gap in the Pareto curve. In Solution 682, the proposed method tried without success to extend the occupied land to reduce fatalities and provide a smooth Pareto curve. In some situations, the new layout may have little differences in safety and economy compared with the original one, and this will make the Pareto curve look continuous. Therefore, the shape of the Pareto curve relies heavily on the actual case. The impact of the discontinuity of industrial FLPs on the solving process will be discussed in Section 6.4.

6 Algorithm comparison

As mentioned in Section 1, there are a number of multi-objective optimization algorithms that can be used to solve industrial facility layout problems (FLPs). In this section, NSGA-II used in our approach will be compared with MOPSO and DMS to solve Case 2. The results from the three algorithms will be analyzed to explore which algorithm is more effective for industrial FLPs, at least for the illustrated case, and the reason for this. The principles of MOPSO and DMS are briefly introduced here for a better understanding of the comparison and the reason.

6.1 Principle of MOPSO

The multi-objective particle swarm optimization (MOPSO) algorithm is based on the classical single-objective PSO algorithm, which approaches the Pareto front based on the movement of particles in the solution space. First, a set of particles representing solutions are randomly generated and evaluated based on the relevant model. Then they are combined with the best particles to obtain ranks. Particles with Rank = 1 are considered as the new best particles. The current position of each particle is compared with its historically best position to determine a new historically best one. If neither of them dominates the other, one is selected randomly.

The velocity and the next position of the particle can be obtained by Eqs. (44) and (45).

$$v_s = W \times Dam^s \times v_{s\text{-}1} + R_1 \times (f_s - p_s) + R_2 \times (g_s - p_s) \tag{44}$$

$$p_{s+1} = p_s + v_s \tag{45}$$

Here, v_{s-1} and v_s are the velocities in the last iteration and current iteration s; p_s and f_s are the current position and historically best position of the particle; g_s is a best position selected randomly; W, Dam, R_1, and R_2 are inertia weight, inertia weight damping rate, personal learning coefficient, and global learning coefficient, respectively, which are pre-set as parameters of MOPSO; and p_{s+1} is the new position of a particle.

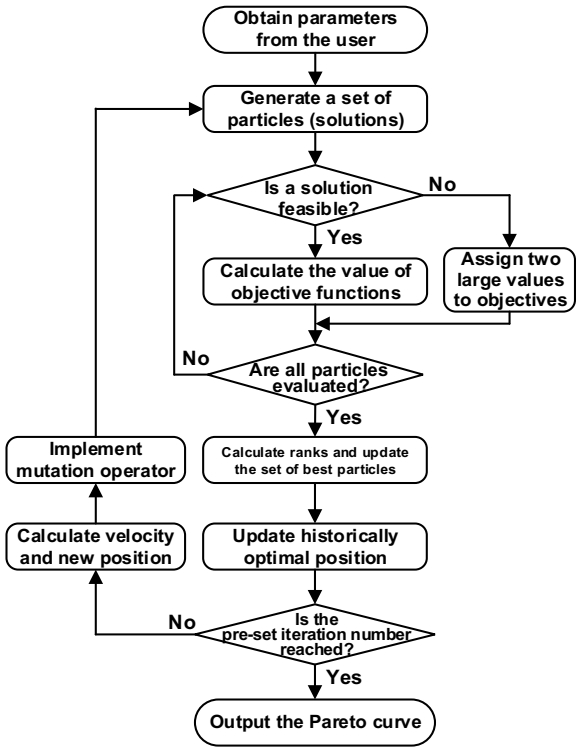

Fig. 15. Flow diagram of MOPSO

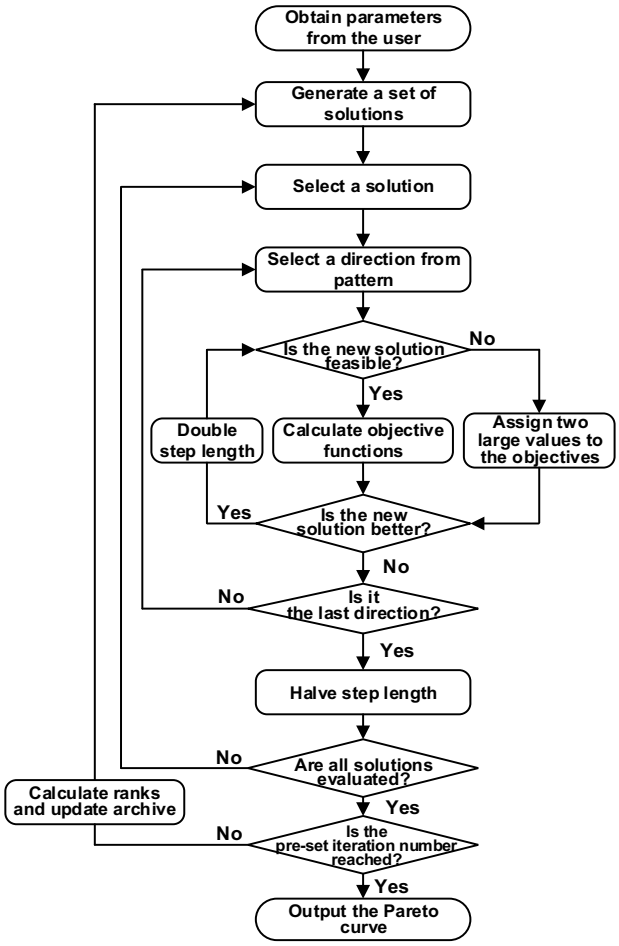

Fig. 16. Flow diagram of DMS

The process described above is repeated for a pre-set number of iterations. The last generation of best

particles is considered as the final solution. A mutation operator may be applied after a new iteration of particles are obtained. The flow diagram of the MOPSO algorithm with a death penalty function is shown in Fig. 15.

6.2 Principle of DMS

The direct multi-search (DMS) method is based on the search/poll paradigm of direct-search methods, which iteratively searches for a better solution in the neighborhood of known solutions to approach the Pareto front. First, DMS generates a set of solutions randomly (called incumbent) and searches in their neighborhood along the directions from pattern one by one. A pattern is a set of orthogonal vectors with *n* dimensions, where *n* is the number of variables. For example, the pattern of a problem with 4 variables is composed of (0, 0, 0, 1), (0, 0, 1, 0), (0, 1, 0, 0), (1, 0, 0, 0), (0, 0, 0, -1), (0, 0, -1, 0), (0, -1, 0, 0), (-1, 0, 0, 0). If a non-dominated point with respect to the current point is found in a direction, DMS doubles the step length and extends the search in the successful direction. If no better solution is found after testing all the directions in the pattern, DMS halves the step length. After searching all neighborhoods of solutions in the incumbent, DMS calculates ranks of the new points together with points in the incumbent and the archive. The archive holds the non-dominated points found so far. Points with Rank = 1 will constitute a new archive. The process described above is repeated until a pre-set number of iterations is reached. The last iteration of the archive is considered as the final solution. The flow diagram of the DMS algorithm with a death penalty function is shown in Fig. 16.

6.3 Optimization results from MOPSO and DMS

The MOPSO and DMS algorithms are implemented for Case 2. The parameters are determined carefully for the two algorithms to ensure a fair comparison. For MOPSO, the number of particles and iterations are set to 4,000 and 1,000 respectively. The significances of these two parameters are similar to the parameters of population size and the number of generations in NSGA-II. Therefore, the same values are used.

For DMS, there are no such similar parameters due to different search mechanisms. The size of the incumbent and the number of iterations are set to 600 and 80 respectively. The calculation time of DMS with these two values (488 min) is already the longest one among the three algorithms as shown below, so the values cannot be increased any further; otherwise, it is unfair for NSGA-II and MOPSO. Also, DMS is a kind of local optimization algorithm, and excessively high values for “incumbent” and “iterations” do not make significant sense in improving the result.

Both programs of MOPSO and DMS were run ten times, and the best results are used for the comparison. Additionally, several sets of different parameters were also tested, and no better solutions were obtained. The Pareto curves from NSGA-II, MOPSO, and DMS are shown in Fig. 17, where they are represented by orange pentagrams, blue asterisks, and green circles, respectively. The numerical results of this comparison are shown in Table 12.

The Pareto curve obtained from NSGA-II is the best and has the most points. The Pareto curve from DMS is the most diverse, that is, it has the most extensive ranges for both objectives with a relatively uniform distribution of points. The Pareto curve from MOPSO is neither optimal nor diverse. All the curves are discontinuous, which is a symptom of the discontinuity of industrial FLPs.

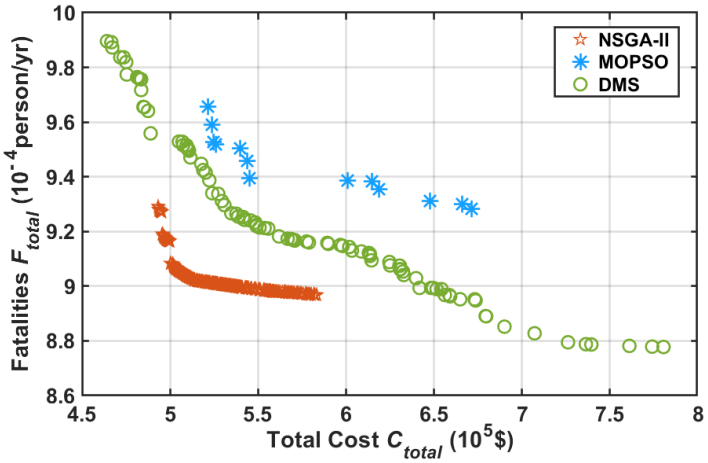

Fig. 17. Pareto curves from NSGA-II, MOPSO, and DMS

Table 12 Numerical results from the comparison

Algorithm	Number of points in Pareto curve	Calculation time (min)	Range of Objective 1 (×10^5 $)	Range of Objective 2 (×10^{-4} person/yr)
NSGA-II	709	421	[4.93, 5.83]	[8.97, 9.29]
DMS	95	488	[4.64, 7.80]	[8.78, 9.90]
MOPSO	13	123	[5.22, 6.71]	[9.28, 9.66]

In terms of calculation time, MOPSO is supposed to have the same calculation time as NSGA-II because the same values have been used for similar parameters. However, MOPSO only spent 123 minutes while NSGA-II spent 421 minutes. The reason is that most of the solutions tried by the MOPSO algorithm are infeasible, and due to the death penalty function, they are given two large values for the two objectives directly, rather than being evaluated as the case is for the proposed model. Therefore, the calculation time is significantly shortened. This explanation is also supported by the small number of points in the Pareto curve from the MOPSO algorithm. It can be deduced that the calculation times for MOPSO and NSGA-II should be the same if other types of penalty functions are used, which evaluate solutions based on the model regardless of whether the solution is feasible or not.

Therefore, NSGA-II seems more effective for industrial FLPs, at least for the illustrated case. This is an experiential and preliminary conclusion. We hope it is helpful for researchers who also focus on industrial FLPs when they are choosing an algorithm.

6.4 Discussion

Many symptoms of the discontinuity of industrial FLPs have appeared in the results from Case 2. In this section, two extreme cases are constructed to illustrate the discontinuity of industrial FLPs and the reason why NSGA-II is better than MOPSO and DMS for industrial FLPs.

Industrial FLPs are severely discontinuous. Feasible regions where the global optimal solution can be located are commonly isolated by infeasible regions. If an algorithm attempts to approach the global optimal solution, it needs to go through an infeasible region. However, MOPSO and DMS do not have the ability to go through infeasible regions and reach another feasible region.

From the principles explained above, the MOPSO algorithm relies on the movement of particles to find the optimal solution. A particle will have a strong tendency to return if it enters an infeasible region because

the position it arrived at is no longer good. This tendency will prevent it from going through infeasible regions and reaching another feasible region.

Case 3 is constructed to demonstrate the isolation of feasible regions by infeasible regions. In order to be able to show the results in a 3-dimentional figure, the case is single-objective and has only two variables. Four plants are fixed in an industrial park. Only one plant is movable, and its coordinates are variables. The objective is to minimize the total length between the center points of the movable plant and the other four plants. The location of the four fixed plants is shown in Fig. 18. The variation of the objective function value with the variables is shown in Fig. 19. The death penalty function is applied for non-overlapping constraints with a penalty value of 100.

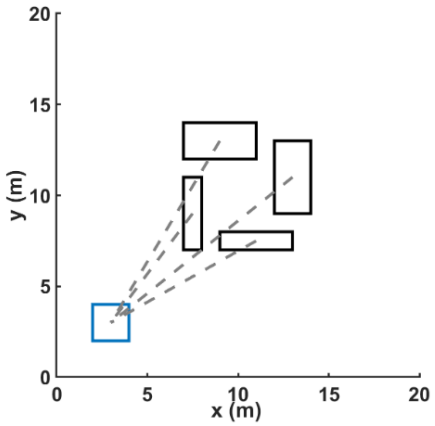

Fig. 18. Plant layout for Case 3

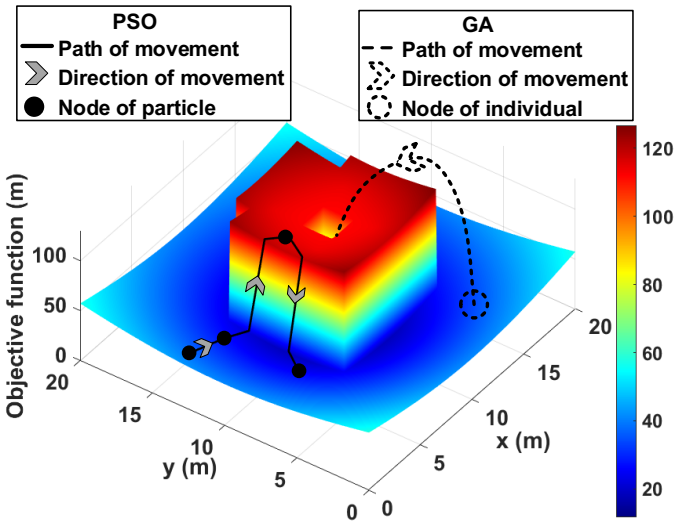

Fig. 19. Objective function values in a solution space

Obviously, the optimal location of the movable plant is the area in the middle surrounded by the other four plants. In Fig. 19, the optimal solution is precisely in the center hole, which is isolated by an infeasible region. For the single-objective PSO, if a particle enters the infeasible region, it tends to return like the solid line path shown in Fig. 19. In contrast, for a single-objective GA, the mutation and crossover operators can make individuals jump rather than move along a path. Therefore, some individuals can jump into the hole like the dashed line path shown in Fig. 19. Once an individual gets into the hole, the selection operator will prevent it from mutation and crossover, that is, it will be kept in the hole and continue to try to find a better solution rather than jump out of the hole. The MOPSO and NSGA-II algorithms are based on the corresponding single-objective algorithms, and therefore they have similar properties as their single-objective versions. Even though the MOPSO algorithm applied in this comparison has a mutation operator, it is still far behind the capability of NSGA-II

Things are a little different for DMS. Case 4 is constructed to illustrate why the direct search method cannot find a better solution or Pareto curve. Case 4 is single-objective and has 4 variables for a visual demonstration. Plant 1 is fixed, while Plants 2 and 3 are movable. The coordinates of Plants 2 and 3 are the variables. The objective is to minimize the total cost consisting of land cost and pipe cost. There is a simple pipe connection between Plants 1 and 3. The location of the plants is shown in Fig. 20. Under the situation shown in Fig. 20, the DMS is trapped in a local optimal solution. For this case, the vectors composing the pattern are shown in Table 13. For each search direction, the physical significance and the test result are also listed.

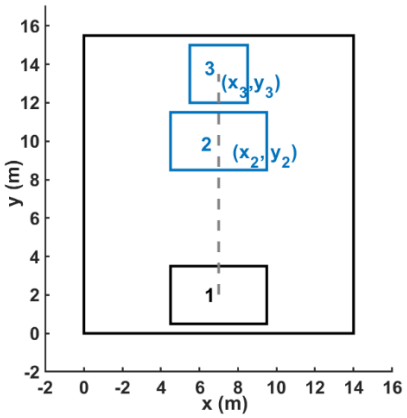

Fig. 20. A location situation for Case 4

Table 13 Pattern and corresponding results of Case 4

Pattern (x_2, y_2, x_3, y_3)	Physical significance	Result
(0, 0, 0, 1)	Move Plant 3 upward	Longer pipe and larger land, failed
(0, 0, 0, -1)	Move Plant 3 downward	Infeasible, failed
(0, 0, 1, 0)	Move Plant 3 right	Longer pipe, failed
(0, 0, -1, 0)	Move Plant 3 left	Longer pipe, failed
(0, 1, 0, 0)	Move Plant 2 upward	Infeasible, failed
(0, -1, 0, 0)	Move Plant 2 downward	No improvement, failed
(1, 0, 0, 0)	Move Plant 2 right	No improvement, failed
(-1, 0, 0, 0)	Move Plant 2 left	No improvement, failed

From Table 13, no matter which direction the algorithm searches along, it cannot find a better solution. The reason is that changing only one variable does not make any improvement. The direction of (0, -1, 0, -1), in which two variables are varied simultaneously, can lead to an improvement. This vector means moving Plants 2 and 3 downwards together. In contrast, both the single-objective GA and NSGA-II change several variables simultaneously to identify a new generation.

This simple case illustrates that industrial FLPs are severely discontinuous. NSGA-II is better than MOPSO and DMS at least in the demonstrated cases, and it seems more effective for industrial FLPs. It should also be noted that the quality of the solution and the shape of the Pareto curve rely heavily on the actual case.

7 Conclusion

In this work, a multi-objective optimization model is proposed for industrial park layout problems, in which a framework of the extended risk map method is developed and integrated. The most significant advantage of the proposed layout model is the ability to provide designers with considerable freedom to achieve different trade-offs between economy and safety, while classical methods with single-objective models can provide only one solution, and designers lose their right to make a trade-off. The extended risk map method considers the uncertainty of meteorological conditions and can ensure the validity of each set of meteorological data. The economy and safety are usually conflicting for industrial layout problems. An economical layout means less land area, shorter pipe, and higher risk, while a safe layout is opposite. The conflict and compromise between economy and safety results in the discontinuity of Pareto curves, which means that sometimes a significant change in layout is necessary to extend the Pareto curve. In addition, by

comparing three different multi-objective optimization algorithms, it is found that the feasible region of industrial facility layout problems is discontinuous. NSGA-II finds the best Pareto curve, while DMS finds the most diverse one. NSGA-II seems more effective for industrial facility layout problems.

8 Acknowledgment

The author of the FLUTE algorithm, Dr. Chris C. N. Chu Iowa State University, and his FLUTE algorithm are greatly acknowledged. Financial support from the Science Foundation of China University of Petroleum, Beijing (No. 2462018BJC004) and the China Scholarship Council (No.201906440120) are also greatly acknowledged.

Nomenclature

Parameters

A_{park}	Area of the industrial park (m^2)
B_{TNT}	Intermediate parameter in TNT equivalent model
$C(x,y,h)$	Concentration of toxic gas in the receptor point (x,y,h) (kg/m^3)
C_{land}	Land cost ($)
$C_{network}$	Network cost ($)
$C_{network,j}$	Cost of pipe network j ($)
$C_{property}$	Property cost ($)
C_{simple}	Simple cost ($)
C_{total}	Total cost ($)
d	Minimum distance between two plants (m)
Dam	Inertia weight damping rate
D_{inner}	Inner diameter (m)
Dom_i	Domain of plant i
D_{outer}	Outer diameter (m)
$D_{x,i,i'}$	Horizontal distance between the boundaries of plants i and i' (m)
$D_{y,i,i'}$	Vertical distance between the boundaries of plants i and i' (m)
E_{TNT}	Explosion energy of TNT (kJ/kg)
f_s	Historically best position of a particle
F_{total}	Expected annual fatalities
g_s	A best position selected randomly
H	Height of the release point (m)
$L_{l,i}$	Length of the long edge of plant i (m)
$L_{s,i}$	Length of the short edge of plant i (m)
$L_{simple,k}$	Length of the simple pipe k (m)
$L_{x,i}$	Length of edge of plant i parallel to x-axis (m)
$L_{y,i}$	Length of edge of plant i parallel to y-axis (m)
M	Mass of explosive material (kg)

M_{TNT}	Equivalent mass of TNT (kg)
N_i	Number of workers in plant *i*
n_{networ}	Number of pipe network
n_{plant}	Number of plants
$n_{segment,j}$	Number of segments in pipe network j
n_{simple}	Number of simple connections
$P(x,y)_{composite,damage}$	probabilities of structural damage in point *(x,y)* (/yr)
$P(x,y)_{composite,death}$	Probabilities of death in point *(x,y)* (/yr)
$P(x,y)_{death,m}$	Probability of death in point (x,y) when an accident occurs in hazard source *m*
$P(x,y)_{demage,m}$	Probability of structural damage in point (x,y) when an accident occurs in hazard source *m*
$P_{accident,m}$	Probability of accident of hazard source *m* (/yr)
$P_{damage,i}$	Probability of structural damage of plant *i* (/yr)
$P_{death,i}$	Annual probability of death in plant *i* (/yr)
p^o	Overpressure (kPa)
p_s	Current position of a particle
Q	Release rate (kg/s)
R	Distance between the receptor point and explosion center (m)
R_1	Personal learning coefficient
R_2	Global learning coefficient
T_{expo}	Exposure time (min)
T_{life}	Lifetime of the industrial park (yr)
U_{land}	Unit price of land ($/m^2)
U_{pipe}	Unit price of a pipe ($/m)
$U_{plant,i}$	Purchase cost of plant *i* ($)
$U_{simple,k}$	Unit price of the simple pipe *k* ($/m)
v_s	Velocity of a particle in iteration *s*
W	Inertia weight
wt_{pipe}	Pipe weight per unit length (kg/m)
x_{upper}	Upper bound in x-axis of the park (m)
x_{lower}	Lower bound in x-axis of the park (m)
$x_{upper,bound}$	Upper bound in x-axis of the available space (m)
$x_{lower,bound}$	Lower bound in x-axis of the available space (m)
$x_{upper,i}$	Upper bound of plant *i* in x-axis (m)
$x_{lower,i}$	Lower bound of plant *i* in x-axis (m)
y_{upper}	Upper bound in y-axis of the park (m)
y_{lower}	Lower bound in y-axis of the park (m)
$y_{upper,bound}$	Upper bound in y-axis of the available space (m)
$y_{lower,bound}$	Lower bound in y-axis of the available space (m)
$y_{upper,i}$	Upper bound of plant *i* in y-axis (m)
$y_{lower,i}$	Lower bound of plant *i* in y-axis (m)
$Y_{cl2,death}$	Probit of death from chlorine
$Y_{ClH,death}$	Probit of death from hydrogen chloride

$Y_{explosion,damage}$	Probit of structural damage from an explosion accident
$Y_{explosion,death}$	Probit of death from an explosion accident
z_{TNT}	Scaled distance (m/kg$^{1/3}$)
α	Yield factor
σ_h	Dispersion coefficient
σ_y	Dispersion coefficient

Subscript

h	Index for pipe segment
i	Index for plants
j	Index for pipe networks
k	Index for simple connections
m	Index for hazard sources
r	Index for constant parameters of TNT equivalent model
s	Index for iterations in MOPSO

Variables

x_i	x coordinate of plant i
y_i	y coordinate of plant i

Binary variable

z_i	Orientation of plant i

Constant parameters

a_{TNT}, b_{TNT}, c_r	Constant parameters in TNT equivalent model
E_1-E_4	Constant parameters for pipe price

References:

1. Meller, R. D.; Gau, K., The facility layout problem: Recent and emerging trends and perspectives. *Journal of Manufacturing Systems* **1996,** 15, (5), 351-366.
2. Guirardello, R.; Swaney, R. E., Optimization of process plant layout with pipe routing. *Computers & Chemical Engineering* **2005,** 30, (1), 99-114.
3. Liu, J.; Liu, J.; Yan, X.; Peng, B., A heuristic algorithm combining Pareto optimization and niche technology for multi-objective unequal area facility layout problem. *Engineering Applications of Artificial Intelligence* **2020,** 89, 103453.
4. Tompkins, J. A.; White, J. A.; Bozer, Y. A.; Tanchoco, J. M. A., *Facilities planning*. 4th ed.; John Wiley & Sons: New York, 2010.
5. Hosseini-Nasab, H.; Fereidouni, S.; Fatemi Ghomi, S. M. T.; Fakhrzad, M. B., Classification of facility layout problems: a review study. *The International Journal of Advanced Manufacturing Technology* **2018,** 94, (1-4), 957-977.
6. Ozyurt, D. B.; Realff, M. J., Geographic and process information for chemical plant layout problems. *Journal of American Institute of Chemical Engineers* **1999,** 45, (10), 2161-2174.
7. Martinez-Gomez, J.; Nápoles-Rivera, F.; Ponce-Ortega, J. M.; Serna-González, M.; El-Halwagi, M. M.,

Siting Optimization of Facility and Unit Relocation with the Simultaneous Consideration of Economic and Safety Issues. *Industrial & Engineering Chemistry Research* **2014,** 53, (10), 3950-3958.

8. Lacksonen, T. A., Static and dynamic layout problems with varying areas. *Journal of the Operational Research Society* **1994,** 45, 59-69.

9. Penteado, F. D.; Ciric, A. R., An MINLP Approach for Safe Process Plant Layout. *Industrial & Engineering Chemistry Research* **1996,** 35, (4), 1354-1361.

10. Alnouri, S. Y.; Linke, P.; El-Halwagi, M. M., Synthesis of industrial park water reuse networks considering treatment systems and merged connectivity options. *Computers & Chemical Engineering* **2016,** 91, 289-306.

11. Wu, Y.; Wang, Y., A Chemical Industry Area-wide Layout Design Methodology for Piping Implementation. *Chemical Engineering Research & Design* **2017,** 118, 81-93.

12. Cormen, T. H.; Leiserson, C. E.; Rivest, R. L.; Stein, C., *Introduction to algorithms*. MIT press: 2009.

13. Wang, R.; Wu, Y.; Wang, Y.; Feng, X.; Liu, M., An Industrial Park Layout Design Method Considering Pipeline Length Based on FLUTE Algorithm. In *Computer Aided Chemical Engineering*, Eden, M. R.; Ierapetritou, M. G.; Towler, G. P., ^Eds. Elsevier: 2018; Vol. 44, pp 193-198.

14. Wu, Y.; Zhang, S.; Wang, Y.; Feng, X., The optimization of area-wide plant layout with piecewise steam pipeline network using parallel genetic algorithm based on GeoSteiner. In *International conference on sustainable energy & environmental protection*, Paisley, UK, 2018.

15. Chu, C.; Wong, Y., FLUTE: Fast lookup table based rectilinear steiner minimal tree algorithm for VLSI design. *IEEE Transactions on Computer-Aided Design of Integrated Circuits and Systems* **2008,** 27, (1), 70-83.

16. Warme, D.; Winter, P.; Zachariasen, M., GeoSteiner. In 2015.

17. Wang, R.; Wang, Y.; Gundersen, T.; Wu, Y.; Feng, X.; Liu, M., A layout design method for an industrial park based on a novel arrangement algorithm – Consideration of pipe network and multiple hazard sources. *Chemical Engineering Science* **2020,** 227, 115929.

18. CCPS, *Guidelines for Siting and Layout of Facilities*. 2nd ed.; John Wiley & Sons: New York, 2018.

19. Latifi, S. E.; Mohammadi, E.; Khakzad, N., Process plant layout optimization with uncertainty and considering risk. *Computers & Chemical Engineering* **2017,** 106, 224-242.

20. AIChE, *Dow's Fire and Explosion Index Hazard Classification Guide (7th Ed.)*. USA: New York, 1994.

21. Patsiatzis, D. I.; Knight, G.; Papageorgiou, L. G., An MILP approach to safe process plant layout. *Chemical Engineering Research and Design* **2004,** A5, (82), 579 – 586.

22. Tugnoli, A.; Khan, F.; Amyotte, P.; Cozzani, V., Safety assessment in plant layout design using indexing approach: Implementing inherent safety perspective Part2—Domino Hazard Index and case study. *Journal of Hazardous Materials* **2008,** 160, (1), 110-121.

23. Lira-Flores, J.; Vázquez-Román, R.; López-Molina, A.; Mannan, M. S., A MINLP approach for layout designs based on the domino hazard index. *Journal of Loss Prevention in the Process Industries* **2014,** 30, 219-227.

24. Jung, S.; Ng, D.; Diaz-Ovalle, C.; Vazquez-Roman, R.; Mannan, M. S., New Approach To Optimizing the Facility Siting and Layout for Fire and Explosion Scenarios. *Industrial & Engineering Chemistry Research* **2011,** 50, (7), 3928-3937.

25. Vázquez-Román, R.; Lee, J.; Jung, S.; Mannan, M. S., Optimal facility layout under toxic release in process facilities: A stochastic approach. *Computers & Chemical Engineering* **2010,** 34, (1), 122-133.

26. Caputo, A. C.; Pelagagge, P. M.; Palumbo, M.; Salini, P., Safety-based process plant layout using genetic algorithm. *Journal of Loss Prevention in the Process Industries* **2015,** 34, 139-150.

27. Alves, D. T. S.; de Medeiros, J. L.; Araújo, O. D. Q. F., Optimal determination of chemical plant layout via minimization of risk to general public using Monte Carlo and Simulated Annealing techniques. *Journal of Loss Prevention in the Process Industries* **2016,** 41, 202-214.

28. Martinez-Gomez, J.; Nápoles-Rivera, F.; Ponce-Ortega, J. M.; Serna-González, M.; El-Halwagi, M. M., Optimization of facility location and reallocation in an industrial plant through a multi-annual framework accounting for economic and safety issues. *Journal of Loss Prevention in the Process Industries* **2015,** 33, 129-139.
29. Deb, K.; Pratap, A.; Agarwal, S.; Meyarivan, T., A fast and elitist multiobjective genetic algorithm: NSGA-II. *IEEE Transactions on Evolutionary Computation* **2002,** 6, (2), 182-197.
30. Coello, C. A. C.; Pulido, G. T.; Lechuga, M. S., Handling multiple objectives with particle swarm optimization. *IEEE Transactions on Evolutionary Computation* **2004,** 8, (3), 256-279.
31. Goldberg, D. E., *Genetic Algorithms in Search, Optimization, and Machine Learning*. Addison-Wesley Publishing Company: 1989.
32. Mezura-Montes, E.; Coello Coello, C. A., Constraint-handling in nature-inspired numerical optimization: Past, present and future. *Swarm and Evolutionary Computation* **2011,** 1, (4), 173-194.
33. Custódio, A. L.; Madeira, J. A.; Vaz, A. I. F.; Vicente, L. N., Direct multisearch for multiobjective optimization. *SIAM Journal on Optimization* **2011,** 21, (3), 1109-1140.
34. Corne, D. W.; Jerram, N. R.; Knowles, J. D.; Oates, M. J. In *PESA-II: Region-based selection in evolutionary multiobjective optimization*, Proceedings of the 3rd Annual Conference on Genetic and Evolutionary Computation, 2001; 2001; pp 283-290.
35. Zitzler, E.; Laumanns, M.; Thiele, L., SPEA2: Improving the strength Pareto evolutionary algorithm. *TIK-report* **2001,** 103.
36. Brazil, M.; Zachariasen, M., *Optimal Interconnection Trees in the Plane*. Springer International Publishing: Switzerland, 2015.
37. Chu, C.; Wong, Y. In *Fast and accurate rectilinear Steiner minimal tree algorithm for VLSI design*, Proceedings of the International Symposium on Physical Design, San Francisco, CA, United states, 2005; Association for Computing Machinery: San Francisco, CA, United states, 2005; pp 28-35.
38. Pasquill, F., The estimation of the dispersion of windborne material. *The Meteorological Magazine* **1961,** 90, (1063), 33-49.
39. CCPS, *Guidelines for Chemical Process Quantitative Risk Analysis*. 2nd Edition ed.; John Wiley & Sons: 2010.
40. Lees, F. P., *Loss Prevention in the Process Industries: Hazard Identification, Assessment and Control*. Butterworth-Heinemann Publisher: Oxford, 2001.
41. Wang, Z., *Handbook of Petrochemical Engineering Design Vol.4*. Chemical Industrial Press: China, Beijing, 2015; p 301-303.
42. Stijepovic, M. Z.; Linke, P., Optimal waste heat recovery and reuse in industrial zones. *Energy* **2011,** 36, (7), 4019-4031.